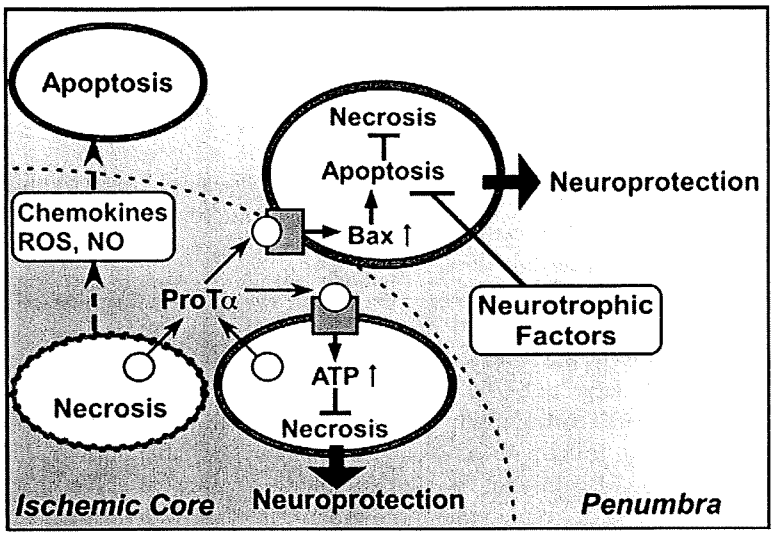


**Figure 3.** Robustness roles of ProTα in the neuroprotection in stroke. The hypothesis depicts the machineries underlying the robustness roles of ProTα through a mechanism of cell death mode switch in cerebral ischemia. In the mild cerebral ischemia, ProTα is first released upon ischemic stress from necrotic cells in the ischemic core. Released ProTα exerts a suppression of the necrosis of neighbored neurons, which plays a role of the early stage of robustness. ProTα at the same time causes apoptosis machineries including caspase 3 activation, which in turn delays the necrosis (through a PARP degradation), as another type of robustness. Expression of neurotrophic factors, such as BDNF or EPO will then occur and block the apoptosis in the penumbra (the late stage of robustness). As the robustness actions of endogenous ProTα seem to be insufficient in the intense ischemia, exogenous administration of ProTα is required for the cure of ischemic brain damages.

which absorbs ProTα.[25] Functional damage was also deteriorated by this antibody treatment, as evaluated by electroretinography (ERG). As ProTα-like immunoreactivities completely disappeared without exception at 3 h after the stress, it is evident that ProTα released upon ischemic stress plays *in vivo* neuroprotective roles.

## Conclusions

The discovery of ProTα initiated investigations into what happens in the event of neuronal necrosis, followed by searches for compounds that inhibit necrosis, based on the detection of its presence in CM from neuronal cultures. The hypothesis that ProTα acts as a "Robustness" or cell death mode switch molecule from uncontrollable necrosis to neurotrophin-reversible apoptosis may provide a promising new strategy for preventing serious damage in stroke (Fig. 3). However, the complete clarification of mechanisms underlying potent neuroprotective actions of ProTα in cerebral and retinal ischemia should wait for the identification of the specific receptor. From this point of view, the involvement of unknown mechanisms independent of $G_{i/o}$-coupled receptors may not be excluded at present. Regarding clinical issues, it is evident that recombinant ProTα itself has unique and potent therapeutic potentials against acute stroke.

## Acknowledgments

Parts of this study were supported by Grants-in-Aid for Scientific Research (to H.U., B: 13470490 and B: 15390028) on priority areas—Research on Pathomechanisms of Brain Disorders (to H.U., 17025031) from the Ministry of Education, Culture, Sports, Science, and Technology (MEXT) and by Health and Labour Sciences Research Grants on Biological Resources and Animal Models for Drug Development.

## Conflicts of interest

The authors declare no conflicts of interest.

## References


1. Ueda, H. 2009. Prothymosin alpha and cell death mode switch, a novel target for the prevention of cerebral ischemia-induced damage. *Pharmacol. Ther.* **123:** 323–333.
2. Qiu, J. *et al.* 2008. Early release of HMGB-1 from neurons after the onset of brain ischemia. *J. Cereb. Blood Flow Metab.* **28:** 927–938.
3. Lai, A.Y. & K.G. Todd. 2006. Microglia in cerebral ischemia: molecular actions and interactions. *Can. J. Physiol. Pharmacol.* **84:** 49–59.
4. Fujita, R. *et al.* 2001. Cell density-dependent death mode switch of cultured cortical neurons under serum-free starvation stress. *Cell. Mol. Neurobiol.* **21:** 317–324.
5. Ueda, H. *et al.* 2007. Identification of prothymosin-alpha1, the necrosis-apoptosis switch molecule in cortical neuronal cultures. *J. Cell Biol.* **176:** 853–862.
6. Pineiro, A., O.J. Cordero & M. Nogueira. 2000. Fifteen years of prothymosin alpha: contradictory past and new horizons. *Peptides* **21:** 1433–1446.
7. Gast, K. *et al.* 1995. Prothymosin alpha: a biologically active protein with random coil conformation. *Biochemistry* **34:** 13211–13218.
8. Matsunaga, H. & H. Ueda. 2006. Voltage-dependent N-Type Ca2+ channel activity regulates the interaction between FGF-1 and S100A13 for stress-induced non-vesicular release. *Cell Mol. Neurobiol.* **26:** 237–246.
9. Matsunaga, H. & H. Ueda. 2006. Evidence for serum-deprivation-induced co-release of FGF-1 and S100A13 from astrocytes. *Neurochem. Int.* **49:** 294–303.
10. Eguchi, Y., S. Shimizu & Y. Tsujimoto. 1997. Intracellular ATP levels determine cell death fate by apoptosis or necrosis. *Cancer Res.* **57:** 1835–1840.
11. Fujita, R. & H. Ueda. 2003. Protein kinase C-mediated cell death mode switch induced by high glucose. *Cell Death Differ.* **10:** 1336–1347.
12. Fujita, R. & H. Ueda. 2003. Protein kinase C-mediated necrosis-apoptosis switch of cortical neurons by conditioned medium factors secreted under the serum-free stress. *Cell Death Differ.* **10:** 782–790.
13. Zong, W.X. & C.B. Thompson. 2006. Necrotic death as a cell fate. *Genes Dev.* **20:** 1–15.
14. Hasegawa, T. *et al.* 2007. Differential localization of aquaporin-2 and glucose transporter 4 in polarized MDCK cells. *Histochem. Cell Biol.* **127:** 233–241.
15. Herrmann, O. *et al.* 2005. IKK mediates ischemia-induced neuronal death. *Nat. Med.* **11:** 1322–1329.
16. Mattson, M.P. & S. Camandola. 2001. NF-kappaB in neuronal plasticity and neurodegenerative disorders. *J. Clin. Invest.* **107:** 247–254.
17. Jiang, X. *et al.* 2003. Distinctive roles of PHAP proteins and prothymosin-alpha in a death regulatory pathway. *Science* **299:** 223–226.
18. Clinton, M. *et al.* 1991. Evidence for nuclear targeting of prothymosin and parathymosin synthesized *in situ*. *Proc. Natl. Acad. Sci. USA* **88:** 6608–6612.
19. Haritos, A.A. *et al.* 1985. Primary structure of rat thymus prothymosin alpha. *Proc. Natl. Acad. Sci. USA* **82:** 343–346.
20. Bianco, N.R. & M.M. Montano. 2002. Regulation of prothymosin alpha by estrogen receptor alpha: molecular mechanisms and relevance in estrogen-mediated breast cell growth. *Oncogene* **21:** 5233–5244.
21. Martini, P.G. *et al.* 2000. Prothymosin alpha selectively enhances estrogen receptor transcriptional activity by interacting with a repressor of estrogen receptor activity. *Mol. Cell Biol.* **20:** 6224–6232.
22. Gomez-Marquez, J. 2007. Function of prothymosin alpha in chromatin decondensation and expression of thymosin beta-4 linked to angiogenesis and synaptic plasticity. *Ann. New York Acad. Sci.* **1112:** 201–209.
23. Fujita, R. & H. Ueda. 2007. Prothymosin-alpha1 prevents necrosis and apoptosis following stroke. *Cell Death Differ.* **14:** 1839–1842.
24. Paul, R. *et al.* 2001. Src deficiency or blockade of Src activity in mice provides cerebral protection following stroke. *Nat. Med.* **7:** 222–227.
25. Fujita, R. *et al.* 2009. Prothymosin-alpha plays a defensive role in retinal ischemia through necrosis and apoptosis inhibition. *Cell Death Differ.* **16:** 349–358.

Cell Death and Differentiation (2010), 1–13

www.nature.com/cdd

# Stress-induced non-vesicular release of prothymosin-α initiated by an interaction with S100A13, and its blockade by caspase-3 cleavage

H Matsunaga[1,2] and H Ueda*,[1]

**The nuclear protein prothymosin-α (ProTα), which lacks a signal peptide sequence, is released from neurons and astrocytes on ischemic stress and exerts a unique form of neuroprotection through an anti-necrotic mechanism. Ischemic stress-induced ProTα release is initiated by a nuclear release, followed by extracellular release in a non-vesicular manner, in C6 glioma cells. These processes are caused by ATP loss and elevated $Ca^{2+}$, respectively. S100A13, a $Ca^{2+}$-binding protein, was identified to be a major protein co-released with ProTα in an immunoprecipitation assay. The $Ca^{2+}$-dependent interaction between ProTα and S100A13 was found to require the C-terminal peptide sequences of both proteins. In C6 glioma cells expressing a Δ88–98 mutant of S100A13, serum deprivation caused the release of S100A13 mutant, but not of ProTα. When cells were administered apoptogenic compounds, ProTα was cleaved by caspase-3 to generate a C-terminal peptide-deficient fragment, which lacks the nuclear localization signal (NLS). However, there was no extracellular release of ProTα. All these results suggest that necrosis-inducing stress induces an extacellular release of ProTα in a non-vesicular manner, whereas apoptosis-inducing stress does not, owing to the loss of its interaction with S100A13, a cargo molecule for extracellular release.**
*Cell Death and Differentiation* (2010) **0**, 000–000. doi:10.1038/cdd.2010.52

Prothymosin-α (ProTα), a nuclear protein, is widely distributed throughout the body and has various intracellular functions in determining life and death.[1,2] ProTα bearing a conventional nuclear localization signal (NLS) is largely localized in the nucleus, and has important functions in the regulation of cell differentiation and proliferation.[1–3] When a cell is subjected to apoptotic stimuli, on the other hand, ProTα is released from the nucleus to the cytosol in which it inhibits apoptosome formation.[4] Thus, ProTα is supposed to have a proliferative function in the nucleus under normal conditions, and a self-defensive function in the cytosol under apoptotic conditions.

We have recently identified ProTα as a unique anti-neuronal necrosis factor in the conditioned medium (CM) of cortical neurons,[5] and discovered its potent neuroprotective functions in cerebral and retinal ischemia.[6,7] This protein is extracellularly released on starving or ischemic stress, and inhibits necrosis by inducing the membrane translocation of glucose transporters, which are endocytosed under ischemic conditions, resulting in an acceleration of necrosis owing to energy crisis.[5] On the basis of pharmacological analyses, ProTα-induced translocation of glucose transporters is mediated by stimulation of a putative $G_{i/o}$-coupled receptor, phospholipase C, and protein kinase C (PKC) $\beta_{II}$. This fact indicates that ProTα has another self-defensive function as an extracellular signal under conditions inducing necrosis.

However, little is known of the mechanisms underlying extracellular ProTα release. Of importance are the facts that the majority of ProTα content in the nucleus is extracellularly released on stress, before membrane disruption,[5] and that ProTα lacks a signal peptide sequence, which is required for sorting to the endoplasmic reticulum (ER)-Golgi system before exocytosis. Therefore, ProTα release seems to proceed in a non-classical or non-vesicular manner under ischemic stress conditions. Here, we report the ischemia-induced nuclear release of ProTα, followed by its interaction with S100A13, a cargo molecule for extracellular release. We also discuss the mechanism underlying the lack of extracellular ProTα release under apoptotic conditions.

## Results

**Serum-deprivation stress-induced non-classical release of ProTα.** ProTα is exclusively localized in the nuclei of various cells, including neurons.[1–3] Starvation stress caused by serum deprivation induced a disappearance of ProTα from neurons and astrocytes, as early as 3 h after the start of primary culture (Figure 1a). Recently, we discovered the release of this protein into the CM of cultured cortical neurons under serum-free starving conditions causing necrosis.[5]

Q1 [1]Division of Molecular Pharmacology and Neuroscience, Nagasaki University Graduate School of Biomedical Sciences, 1-14 Bunkyo-machi, Nagasaki 852-8521, Japan
*Corresponding author: H Ueda, Division of Molecular Pharmacology and Neuroscience, Nagasaki University Graduate School of Biomedical Sciences, 1-14 Bunkyo-machi, Nagasaki 852-8521, Japan. Tel: +81 95 819 2421; Fax: +81 95 819 2420; E-mail: ueda@nagasaki-u.ac.jp
[2]Current address: Department of Applied Life Science, Faculty of Biotechnology and Life Science, Sojo University, Ikeda 4-22-1, Kumamoto 860-0082, Japan
**Keywords:** non-vesicular release; prothymosin-α; S100A13; necrosis and apoptosis
**Abbreviations:** BDNF, brain-derived neurotrophic factor; BSA, bovine serum albumin; CM, conditioned medium; DAMPs, damage-associated molecular patterns; 2-DG, 2-deoxy-D-glucose; ER, endoplasmic reticulum; FGF, fibroblast growth factor; FRET, fluorescence resonance energy transfer; HMGB1, high-mobility group box1; NLS, nuclear localization signal; OU, oscillation unit; PKC, protein kinase C; ProTα, prothymosin-α; QCM, quartz crystal microbalance
Received 06.8.09; revised 14.1.10; accepted 26.1.10; Edited by L Greene

Journal: CDD ☐ Disk used Despatch Date: 3/5/2010
Article : npg_cdd_cdd201052 Pages: 1–14 OP: XXX ED: XXX CE: XXX Graphic: 2,5,6 col

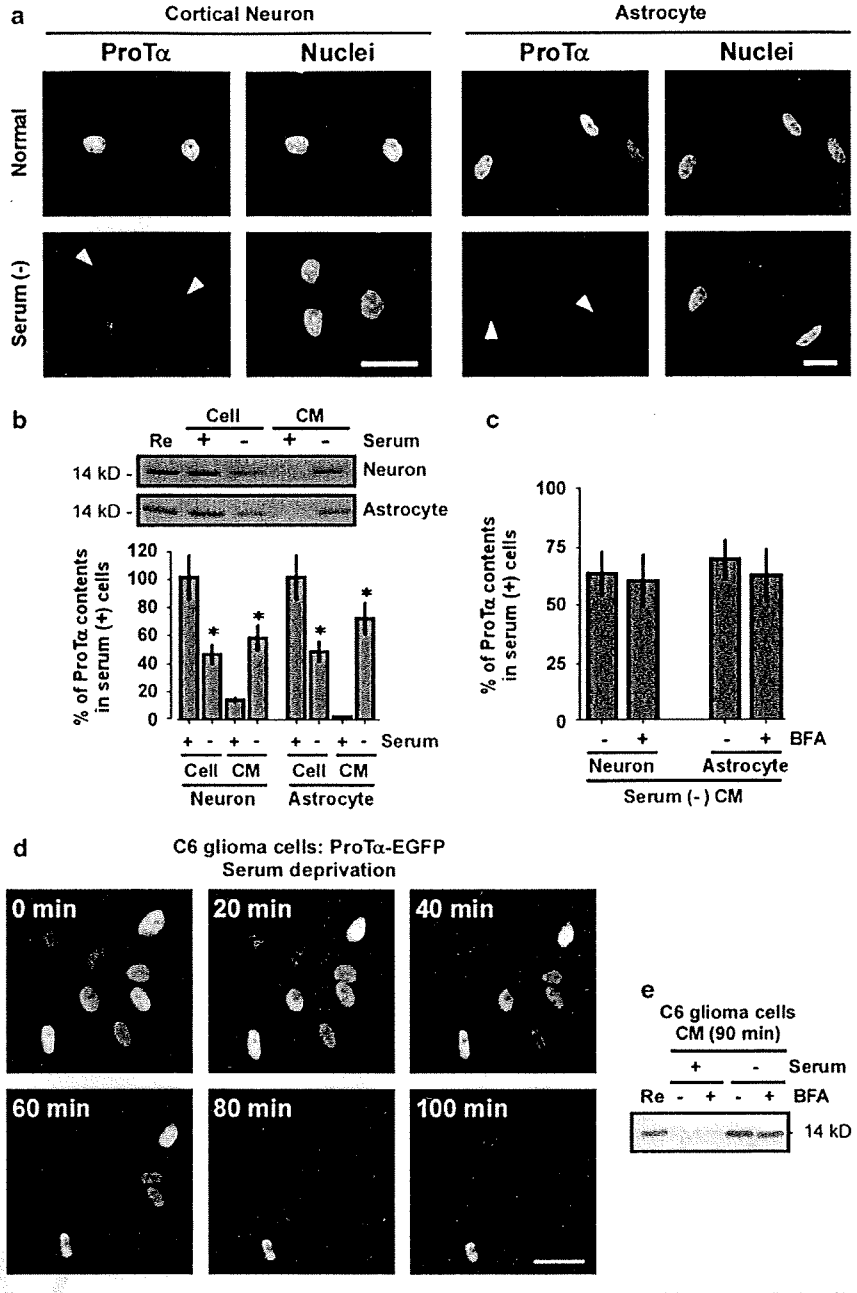


**Figure 1** Serum-deprivation stress induced the brefeldin-A-insensitive non-classical extracellular release of ProTα. (**a**) Altered distribution of ProTα in cortical neurons and astrocytes. Cells were fixed for immunocytochemistry 3 h after serum-deprivation stress, indicated as serum (−). Arrowheads denote the nuclei of cells showing ProTα release. (**b**) ProTα release in cortical neurons and astrocytes induced by serum (−) stress. ProTα, a highly acidic protein, was purified from $5 \times 10^5$ cells and their CM using a phenol extraction procedure, and visualized with Coomassie brilliant blue. Data represent the means ± S.E.M. of five independent experiments [$^*P = 0.01$, *versus* the corresponding serum (+) treatment]. (**c**) Characterization of brefeldin A-insensitive non-classical extracellular release of ProTα. Brefeldin A (BFA; 8 μg/ml) was added to the culture of cortical neurons and astrocytes 12 h before serum deprivation. CM samples ($n = 5$) were used for the purification of ProTα. (**d**) Real-time imaging of serum-deprivation stress-induced ProTα release. ProTα-EGFP stably expressed in C6 glioma cells was released on serum-deprivation stress. (**e**) Serum-deprivation stress-induced ProTα release in a BFA-insensitive manner. CM samples from C6 glioma cells culture were collected at 90 min after serum-deprivation stress (90 min). Scale bars represent 20 μm. Re: recombinant rat ProTα

As shown in Figure 1b, when serum-derivation stress was given to neurons or astrocytes, the amounts of ProTα in both cell types markedly decreased at 3 h. On the other hand, the ProTα levels in the CM of both cell types in the presence of serum were negligible. However, the serum-deprivation stress caused a significant extracellular release of ProTα from both cell types. Brefeldin A, a blocker of protein transport from the ER to the Golgi apparatus, did not affect



NPG.CDD.CDD201052

ProTα release (Figure 1c), suggesting that the manner of release differs from conventional vesicular release. Extracellular release of ProTα was also observed in a rat astroglial C6 glioma cell line after serum deprivation. In C6 glioma cells expressing ProTα-EGFP, the serum-deprivation stress-induced decrease of fluorescence in nuclei started as early as 20 min after serum deprivation, and complete disappearance was observed at 80 min, although a small population of cells (below 5%) still retained fluorescence (Figure 1d). However, no significant fluorescence signal was observed in the cytosol at these time points, suggesting that stress-induced nuclear export of ProTα is a rate-limiting step in the non-classical extracellular release of ProTα. As seen with primary neurons and astrocytes, brefeldin A did not affect the serum-deprivation stress-induced release of native ProTα release from C6 glioma cells (Figure 1e).

**ATP-dependent nuclear localization of ProTα.** We have earlier reported that serum-free starvation stress causes a rapid decrease in cellular ATP levels, leading to necrosis and extracellular ProTα release from the nucleus.[5] As shown in Figure 2a, the addition of 2-deoxy-D-glucose (2-DG) to cultured C6 glioma cells in serum-containing medium caused a rapid decrease in ATP levels. When the subcellular localization of ProTα was examined (Figure 2b), the addition of 2-DG to cells without serum-starvation stress decreased the number of cells showing nuclear localization of ProTα, and increased the number showing cytosol localization. However, no significant extracellular ProTα release was observed. On the other hand, serum-deprivation treatment decreased the number of cells showing nuclear localization and increased the number showing extracellular release. Thus, these results suggest that the loss of cellular ATP induces the transport of ProTα from the nucleus to cytosol, but is not sufficient to cause extracellular release of ProTα from the cytosol.

We studied the machinery underlying nucleus-to-cytosol export. When Alexa Fluor488-labeled ProTα and Alexa Fluor568-bovine serum albumin (BSA) were co-injected into the cytosols of C6 glioma cells, Alexa Fluor488-ProTα was rapidly localized to the nucleus, within 10 min, whereas Alexa Fluor568-BSA remained in the cytosol (Figure 2c, upper left 4 panels). Treatment of cells with 2-DG abolished the nuclear localization of Alexa Fluor488-ProTα and redistributed it throughout the cell (Figure 2c, upper middle 4 panels). This re-distribution was completely reversed by co-injection of ATP (Figure 2c, upper right 4 panels). On the other hand, serum deprivation caused a re-distribution of ProTα from nucleus to cytosol, but did not result in extracellular release in the presence of amlexanox, which inhibits the release of proteins lacking a signal peptide sequence[8–11] (Figure 2c, lower panels). Similarly, co-injection of ATP reversed the nucleus-to-cytosol export. Thus, it is evident that nuclear localization of ProTα is closely related to the cellular ATP level.

Importin α has an important function in the nuclear localization of proteins possessing an NLS. For the sustained localization of such proteins, importin α should be released into the cytosol for repeated use. The GTP-bound form of Ran, a small GTP-binding protein, is known to execute this importin recycling process.[12] Therefore, the loss of cellular ATP is expected to impair the nuclear localization of ProTα owing to difficulty maintaining the GTP-bound state of Ran. Indeed, the nuclear localization of ProTα-EGFP was clearly impaired by injection of anti-importin α IgG into C6 glioma cells (Figure 2d). However, the nuclear levels of ProTα were not affected by leptomycin B, an inhibitor of the nuclear export receptor CRM1 (data not shown). When wheat germ agglutinin, an inhibitor of the nuclear pore complex, was injected into the nuclei of C6 glioma cells, ProTα was redistributed throughout the cells (Figure 2e). All of these findings suggest that ProTα is localized in the nucleus through an ATP-dependent importin-NLS mechanism,[13] and that nucleus-to-cytosol export owing to loss of ATP occurs through passive diffusion.

**Stress-induced extracellular co-release of ProTα with S100A13.** When the CM from serum-deprived C6 glioma cells was immunoprecipitated with anti-ProTα IgG, two significant protein bands were stained by CBB (Figure 3a). The upper band was identified as ProTα by immunoblot using an acidic protein transfer procedure.[14] The lower band, at approximately 10 kDa, was identified by matrix-assisted laser desorption/ionization-time of flight (MALDI-TOF) (five peptides, 57.1% coverage) followed by MS/MS sequence-tag analysis using the NCBI protein database, as S100A13, a member of the $Ca^{2+}$-binding S100 family.[15–17] Immunoblotting also confirmed that this protein is identical to S100A13.

As shown in Figure 3b, naturally occurring ProTα is localized within nuclei, whereas S100A13 is evenly distributed throughout cells. When cultured cells were deprived of serum, both ProTα and S100A13 were completely lost from cells at the time point of 3 h. The cellular loss of S100A13 and ProTα was also blocked by amlexanox, a potent inhibitor of S100A13.[8–11,18] Quantitative immunoblot analysis confirmed that amlexanox abolished the serum-deprivation stress-induced extracellular release of ProTα (Figure 3c).

**Protein–protein interaction between ProTα and S100A13.** The interaction between ProTα and S100A13 was characterized by use of various deletion mutants of both proteins. In this study, GST-tagged ProTα and *Strep*-tagII-S100A13 were used (Figure 4a). The addition of *Strep*-tagII-S100A13 to GST-ProTα immobilized on the sensor tip of a quartz crystal microbalance (QCM) decreased the quartz oscillation, as quantified by the oscillation unit (OU: $\Delta F$ in Hz), which represents the degree of interaction between the two proteins, as reported earlier.[19] The interaction between proteins was enhanced in the presence of $Ca^{2+}$, but not in the presence of $Mg^{2+}$ or $Cu^{2+}$, and this enhancement was $Ca^{2+}$ dependent in the range 0.1–200 μM (Table 1; Figure 4b). As the $Ca^{2+}$-dependent interaction was further enhanced by the addition of $Cu^{2+}$ (Table 1), which has substantial binding affinity for S100A13, we used the addition of both $Ca^{2+}$ and $Cu^{2+}$ (100 μM and 100 nM, respectively) to determine the best ionic conditions for the interaction between GST-ProTα and *Strep*-tagII-S100A13. From the kinetic analysis,[19] the saturated $OU_{max}$ for the interaction of *Strep*-tagII-S100A13 with immobilized GST-ProTα (430 fmol) was 201.44 ± 3.53 OU, which corresponds to



NPG.CDD.CDD201052

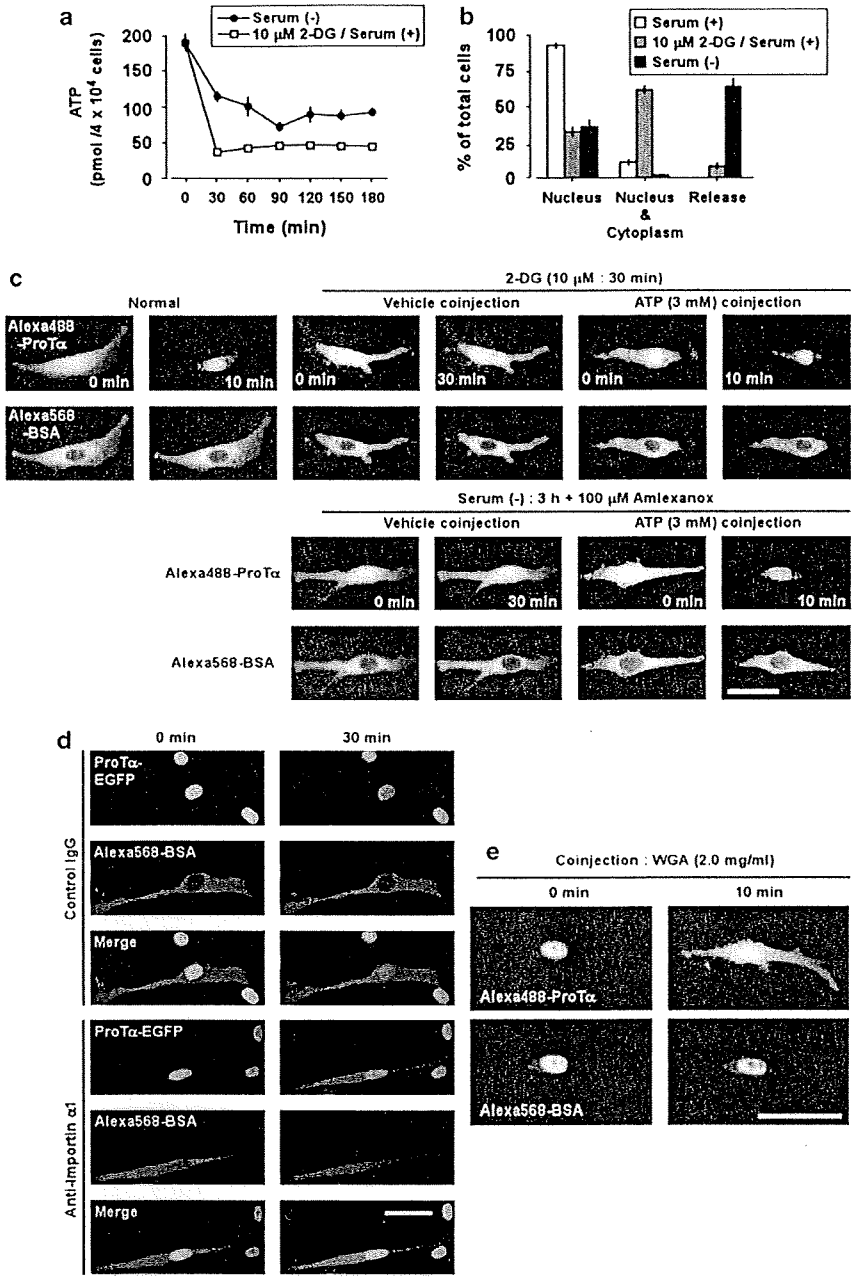


**Figure 2** Mechanism underlying the nuclear transport of ProTα. (**a**) Decrease in intracellular ATP levels induced by serum-deprivation stress. Time courses of intracellular ATP levels were measured in ProTα-EGFP stably expressing C6 glioma cells subjected to serum-deprivation stress or treated with 2-DG (10 μM, with serum). (**b**) Altered distribution of ProTα-EGFP by serum (−) or 2-DG treatments (3 h). Distribution of ProTα-EGFP was measured after fixation of C6 glioma cells and visualization of nuclei with Hoechst 33342. Data represent the means ± S.E.M. of 4–6 independent experiments. (**c**) ATP-induced recovery of nuclear import of ProTα after 2-DG treatment or serum (−) stress in the presence of amlexanox (100 μM). Alexa Fluor488-ProTα and Alexa Fluor568-BSA, with or without ATP (3 mM in a needle), were co-injected into cytoplasm. (**d**) Nuclear import of ProTα mediated by importin α. Importin α, a nuclear transport receptor, binds to classical NLS-containing proteins and links them to the nuclear pore complex. Re-distribution of ProTα-EGFP after cytosolic co-injection of anti-importin α IgG (0.1 μg/ml in a needle) and Alexa Fluor568-BSA. (**e**) Passive diffusion of ProTα as a nuclear export mechanism. Injection of wheat germ agglutinin (WGA, 2.0 mg/ml in a needle) into the nucleus induced a re-distribution of ProTα throughout the cell. Scale bars represent 20 μm

435.63 ± 7.63 fmol. Therefore, it is evident that ProTα and S100A13 interact at a ratio of 1 : 1.

The C-terminal domains of several types of S100 family proteins are reported to interact with various target proteins.[16] Among these proteins, S100A13 has a unique C-terminal 11-amino-acid sequence (RKEKVLAIRKK), which contains as many as six basic amino acids. In the QCM analysis, *Strep*-tagII-S100A13 lacking this C-terminus (amino-acids



NPG.CDD.CDD201052

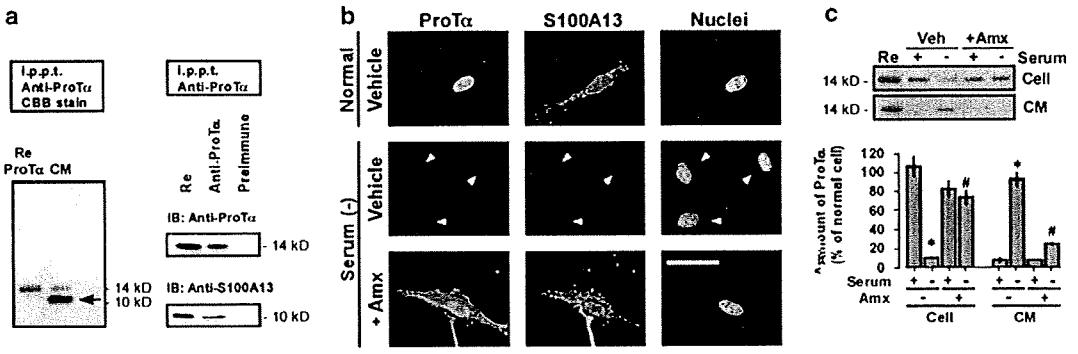


**Figure 3** Identification of S100A13 co-released with ProTα on serum-deprivation stress. (**a**) S100A13 is a major protein interacting with extracellular ProTα. CM from serum-deprived C6 glioma cells (3 h) was subjected to immunoprecipitation with anti-ProTα or pre-immune IgG. Lower band was identified as S100A13 (arrow). Re, recombinant rat ProTα; IB, immunoblot. (**b**) Blockade of stress-induced extracellular release of ProTα and S100A13 by amlexanox. Cells were subjected to serum-deprivation stress (3 h) in the presence or absence of amlexanox (Amx: 100 μM, pretreatment for 30 min). Arrowheads denote the nuclei of cells showing ProTα and S100A13 release. Scale bar represents 20 μm. (**c**) Biochemical analysis of amlexanox-induced blockade of serum-deprivation stress-induced extracellular release of ProTα. ProTα in the CM and residual cells was measured by immunoblot. CM was immunoprecipitated with anti-ProTα IgG. Data represent the means ± S.E.M. of five independent experiments [* and $^{\#}P<0.01$, *versus* the corresponding serum (+) and the corresponding Amx (−) treatment, respectively]

88–98) showed no significant interaction with ProTα (Figure 4c). On the other hand, in the experiments using immobilized *Strep*-tagII-S100A13, the C-terminal deletion mutants ProTα (Δ79–112) and ProTα (Δ102–112) showed decreased potency for interaction (association rate constant: $k_a$), whereas the N-terminal deletion mutants ProTα (Δ1–68) and ProTα (Δ1–86) did not (Figure 4d). As the C-terminal peptide ProTα (amino-acids 102–112; TKKQKKTDEDD), but not its reverse peptide (DDEDTKKQKKT), inhibited the interaction between GST-ProTα and *Strep*-tagII-S100A13 (Figure 4e), the C-terminal sequence appears to have a crucial function in this interaction. On the contrary, the N-terminal region is presumed to have an unidentified regulatory function in this interaction.

**Interaction between ProTα and S100A13 is required for the extracellular release of ProTα.** To confirm that the stress-induced extracellular release of ProTα depends on the ProTα–S100A13 interaction, we established C6 glioma cells stably expressing *Strep*-tagII-S100A13 Δ88–98, which lacks affinity for ProTα. In the immunocytochemical study, serum-deprivation stress caused an extracellular release of both ProTα and *Strep*-tagII-S100A13 full-length mutant from C6 glioma cells (Figure 5a, left panels, and 5b). However, with the *Strep*-tagII-S100A13 Δ88–98 mutant, serum-deprivation stress caused the release of the mutant protein, but not ProTα (Figure 5a, right panels, and 5b). This finding suggests that the C-terminal basic residue-rich domain of S100A13 is required for the interaction with ProTα in living cells, and that S100A13 has a function as a cargo molecule involved in the extracellular export of ProTα. To identify the intracellular locales of interaction between ProTα and S100A13, we performed *Strep*-tagII pull-down assay using nuclear and cytosolic fractions from C6 glioma cells stably expressing *Strep*-tagII-S100A13 (Figure 5c). In the absence of stress, there was no interaction between *Strep*-tagII-S100A13 and ProTα in either nuclear or cytosol fraction. Under the serum-deprivation stress, however, a significant interaction was observed in the cytosol fraction, but not in the nuclear one. The level of co-precipitated ProTα in the cytosol was decreased in a time-dependent manner in the range between 1 and 3 h, possibly because of the loss of cytosolic ProTα by extracellular release of both proteins. To evaluate the ProTα–S100A13 interaction in living cells, we performed fluorescence resonance energy transfer (FRET) analysis. However, the representative FRET analysis using a pair of CFP and YFP was not successful, because the YFP-fused ProTα showed an abnormal distribution. Instead, we attempted to assess the interaction between ProTα-EGFP and DsRed2-S100A13 in the presence of amlexanox, which has no direct effect on their interaction (Table 1). In addition, we performed using phenol red-free DMEM, which does not decrease the survival activity of C6 glioma cells under serum-deprivation condition (Supplementary Figure S1). In the cell population, FRET analysis in the presence of amlexanox, the serum-deprivation stress-induced interaction between ProTα and S100A13 (Figure 5d), and ProTα and S100A13 were redistributed throughout the cell (Figure 5g). To calculate the FRET efficiency, we performed acceptor photo-bleaching. When the acceptor (DsRed2-S100A13) was earlier bleached, serum-deprivation stress did not cause elevation of FRET ratio; however, ProTα and S100A13 were also redistributed throughout the cell (Figure 5d and g). Next, we performed the single cell FRET analysis in the absence of amlexanox. As shown in Supplementary Figure S2a, the FRET ratio in the cytosol was rapidly increased at 80 min after serum deprivation, whereas then gradually decreased, possibly because of the extracellular release of ProTα–S100A13 complex. In accord with this observation, the fluorescence intensity derived from donor ProTα-EGFP decreased at 80 min, whereas the one derived from acceptor DsRed2-S100A13 transiently increased (Supplementary Figure S2b). These results strongly suggest that the interaction between ProTα-EGFP and DsRed2-S100A13 occurs in the cytosol. As shown in Figure 5e, the serum-deprivation stress-induced interaction between ProTα and S100A13 was abolished by the C-terminal (102–112) peptide of ProTα, but not by the



NPG.CDD.CDD201052

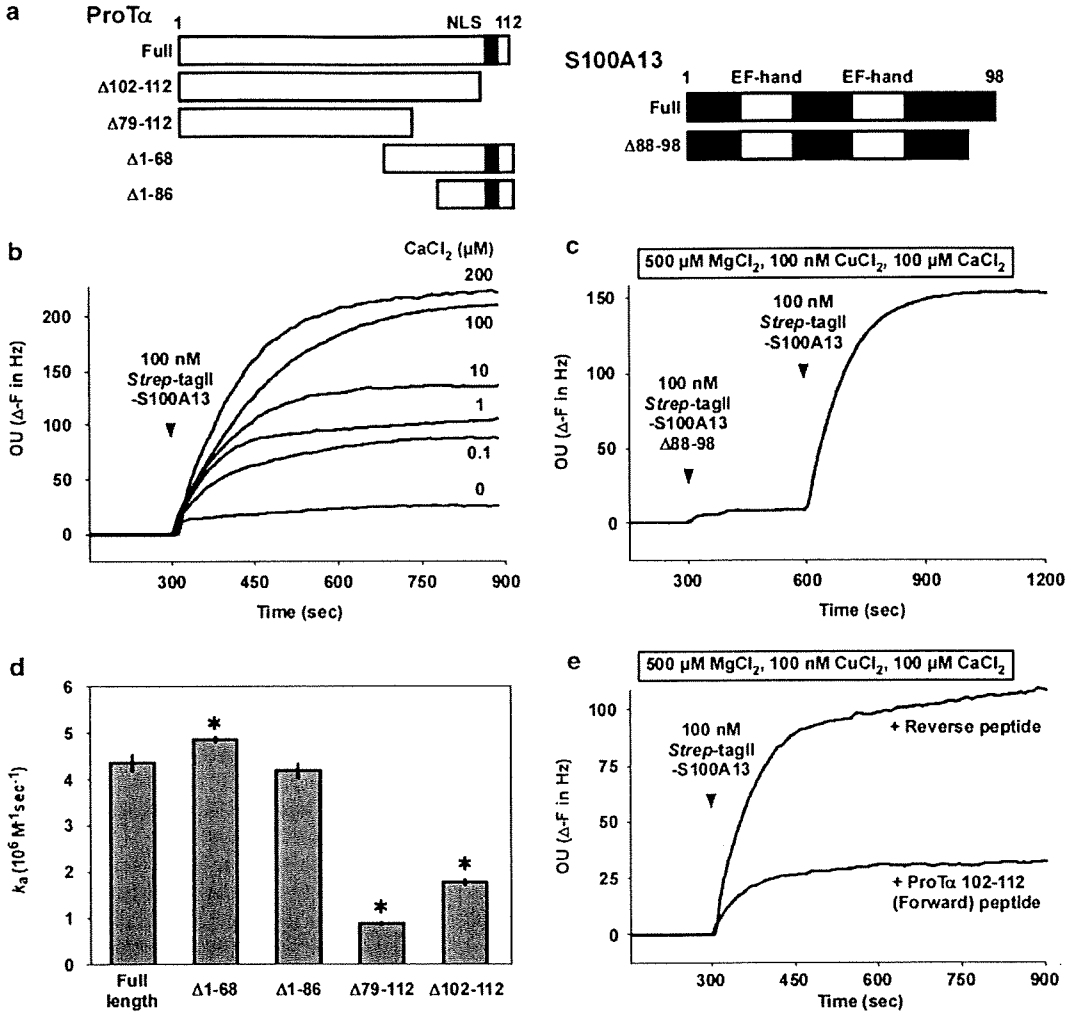


**Figure 4** Biochemical interaction between GST-ProTα and *Strep*-tagII-S100A13, evaluated by QCM. (a) ProTα and S100A13 mutant constructs. (b) The interaction between GST-ProTα and *Strep*-tagII-S100A13 occurs in a $Ca^{2-}$ concentration-dependent manner. The time course of the interaction in the presence of various concentrations of $Ca^{2+}$ (0–200 $\mu$M) was measured. (c) Loss of interaction between S100A13 lacking the C-terminal region (Δ88–98) and ProTα. (d) Loss of interaction between GST-ProTα deletion mutants lacking C-terminal regions and *Strep*-tagII-S100A13. Data represent the means ± S.E.M. of five independent experiments (*$P<0.05$, *versus* full length). (e) Interference by ProTα C-terminal forward peptide (amino-acids 102–112). Arrowheads represent the application points of *Strep*-tagII-S100A13 mutants

**Table 1** The association rate constant ($k_a$) and dissociation constant ($K_D$) value of *Strep*-tagII-S100A13 for GST-ProTα in the QCM assay

| | $Mg^{2+}$ ($\mu$M) | $Ca^{2+}$ ($\mu$M) | $Cu^{2+}$ ($\mu$M) | Amlexanox (100 $\mu$M) | $k_a$ ($10^4$/M/s) | $K_D$ ($10^{-8}$ M) |
|---|---|---|---|---|---|---|
| A | 0 | 0 | 0 | – | 1.98 ± 0.28 | 21.19 ± 3.43 |
| B | 100 | 0 | 0 | – | 1.83 ± 0.31 | 27.66 ± 6.52 |
| C | 0 | 100 | 0 | – | 10.03 ± 0.14** | 6.98 ± 0.09** |
| D | 0 | 0 | 100 | – | 3.40 ± 0.52 | 13.62 ± 3.03 |
| E | 500 | 100 | 0 | – | 7.01 ± 0.21 | 5.72 ± 0.17 |
| F | 500 | 100 | 0.1 | – | 9.46 ± 0.23* | 3.20 ± 0.68* |
| G | 500 | 100 | 0 | + | 6.84 ± 0.06 | 5.89 ± 0.18 |
| H | 500 | 100 | 0.1 | + | 9.88 ± ± 0.43* | 4.38 ± 0.20* |

The interaction between ProTα and S100A13 was in a $Ca^{2+}$-dependent manner. The interaction was analyzed by both GST-ProTα and *Strep*-tagII-S100A13. GST-ProTα was immobilized on the anti-GST antibody-coated sensor chip, hence orientation of ProTα (host sample) was fixed. The $k_a$ and $K_D$ values were obtained by the analysis using cumulative application of *Strep*-tagII-S100A13 (guest sample). $Cu^{2+}$ potentiated the $Ca^{2+}$-dependent interaction between GST-ProTα and *Strep*-tagII-S100A13. Amlexanox did not affect this interaction. Each experiment was analyzed in interaction buffer. The data shown are mean ± S.E.M. of 3–5 independent experiments. *$P<0.05$ and **$P<0.01$ *versus* corresponding control (A and E)



NPG.CDD.CDD201052

reverse peptide. The treatment with C-terminal peptide inhibited the serum-deprivation-induced extracellular release of ProTα, but not S100A13, whereas the reverse peptide did not inhibit the extracellular release of either protein (Figure 5h, upper 6 panels).

**$Ca^{2+}$ influx is involved in the extracellular release of ProTα based on the interaction with S100A13.** In the FRET analysis (Figure 5f), the serum-deprivation stress-induced interaction between ProTα and S100A13 was abolished when the cells were treated with EGTA or BAPTA-AM, extracellular and intracellular $Ca^{2+}$-chelating agents, respectively. The serum-deprivation-induced loss of these proteins was also abolished by EGTA or BAPTA-AM (Figure 5h, lower 4 panels).

**Caspase-catalyzed cleavage of ProTα inhibits the stress-induced extracellular release.** When C6 glioma cell culture was carried out in various concentrations of serum, significant depletion of ProTα was observed in the absence of serum, but not in the presence of 2 or 10% serum (Figure 6a, upper 6 panels, and 6b). When staurosporine, tunicamycin, and etoposide, which are known to induce apoptosis, were added to 2% serum medium, ProTα was redistributed throughout the cell (Figure 6a, middle 6 panels). However, these apoptogenic compounds did not cause any significant extracellular release of ProTα, but led to the production of large amounts of a smaller ProTα fragment (Figure 6b). These re-distribution and fragmentation of ProTα were in a caspase-3 inhibitor zDEVD-fmk-reversible manner (Figure 6a, lower 6 panels and 6b). On the other hand, these compounds did not affect intracellular ATP levels (Supplementary Figure S3).

When rat ProTα was treated with active caspase-3, a 13 kDa protein band was time dependently generated in a zDEVD-fmk-reversible manner (Figure 6c). This finding is consistent with reports that human ProTα has three over-lapping caspase-3 cleavage sites, 94DDED97, 95DEDD98, and 97DDVD101,[20,21] immediately upstream of the NLS moiety in its C-terminus, and that this fragment lacks an NLS moiety KKQK, which is present in rat ProTα at amino-acid positions 103–106. To identify the cleavage sites of rat ProTα by active caspase-3, we performed MALDI-TOF analysis. As shown in Figure 6e, MALDI-TOF analysis revealed that the molecular mass of purified ProTα in naive C6 glioma cells was 12259.99, which corresponds to N-terminal serine acetylated full-length size (Ac2-112), whereas ProTα-like molecule in apoptogenic staurosporine-treated cells was 10480.39 or 10596.43, which corresponds to C-terminal truncated ProTα Ac2-97 or Ac2-98, respectively. Tunicamycin or etoposide treatments also showed similar results (data not shown). Next, we tried to characterize the cleavage region of recombinant rat ProTα (rrProTα) by caspase-3 by use of peptide mass fingerprinting analysis. In this experiment, rrProTα was incubated with or without active rat caspase-3, followed by a separation with SDS-PAGE, in-gel digestion of protein bands with trypsin and MALDI-TOF analysis (Figure 6f). In the absence of incubation of active rat capase-3 (blue peaks), two peaks with molecular mass of 1131.15 and 1479.66 were identified as a.a.22–31 and a.a.91–103 peptides, respectively. However, in its presence (black peaks), there were new peaks with 792.47 and 907.41, corresponding to a.a.91–97 and a.a.91–98 peptides, respectively, but the peak with 1479.66 disappeared. Furthermore, the digestion of synthetic rat ProTα C-terminal 93–112 polypeptide by caspase-3 produced two peaks with molecular mass of 1678.88 and 1794.01, which correspond to a.a.99–112 and a.a.98–112 peptides, respectively (Figure 6g). All these results indicate that rat ProTα has the two over-lapping cleavage sites by caspase-3 (Figure 6d). Accordingly, ProTα likely loses its NLS moiety under apoptotic conditions. This view is supported by the finding that immunoreactive ProTα is no longer localized in the nucleus after treatment of cells with apoptogenic compounds (Figure 6a). On the basis of the finding that the ProTα fragment was not released from cells, this C-terminal region appears to be essential for the extracellular release of ProTα.

## Discussion

The nuclear protein ProTα currently attracts the interest of investigators in terms of life and death decisions in various cell types. In the nucleus, this protein epigenetically stimulates cell proliferation by binding to histones,[22] p300 histone acetyl-transferase,[23] and CREB-binding protein.[24] ProTα also inhibits estrogen receptor transcriptional activity by binding to its repressor,[25] and binds to Keap1 to release Nrf2, which in turn upregulates various kinds of anti-oxidant enzymes important for survival.[26] Under the apoptotic conditions, it inhibits apoptosome formation.[4] Most recently, we discovered this protein as an anti-necrosis factor in the CM of cultured cortical neurons under serum-free starving conditions causing necrosis.[5] Extracellular ProTα completely inhibits neuronal necrosis, but causes apoptosis in a different manner in cultured neurons.[27–29] However, after stroke, endogenous neurotrophins, such as brain-derived neurotrophic factor (BDNF) or erythropoietin, have been found to inhibit the apoptosis induced by exogenously administered ProTα.[6] In the retinal ischemia model, the ischemic stress depletes ProTα from the retinal cells, and the intravitreous pretreatments with anti-ProTα IgG or antisense oligodeoxynucleotide against ProTα deteriorated the ischemic damage.[7] Therefore, it is evident that ProTα is extracellularly released from nuclei on ischemic stress, and that it exerts endogenous neuroprotective functions.

Polypeptide secretion has largely been defined as a process of exocytosis through the fusion of vesicles containing bioactive substances to the plasma membrane. In the representative vesicular secretion pathway, polypeptides that possess a signal peptide sequence in their N-terminal region are sorted to the ER-Golgi system to be processed by exocytosis.[30,31] However, several polypeptides possess extracellular functions despite lacking a signal sequence. The extracellular release of such polypeptides has to proceed through ER-Golgi-independent or non-vesicular (so-called non-classical) routes. It should be noted that these polypeptides showing non-classical extracellular release in general have significant functions in the life and death decisions of cells, as seen in the cases with angiogenic growth factors, inflammatory cytokines, extracellular matrix



NPG.CDD.CDD201052

growth factors, viral proteins, and parasite surface proteins.[32,33] Unlike vesicular release, this type of release is caused by non-physiological stressful stimuli, which may cause rapid cell death. A series of pioneering studies by Maciag and his coworkers led to the hypothesis that S100A13 has key functions in the so-called non-classical extracellular

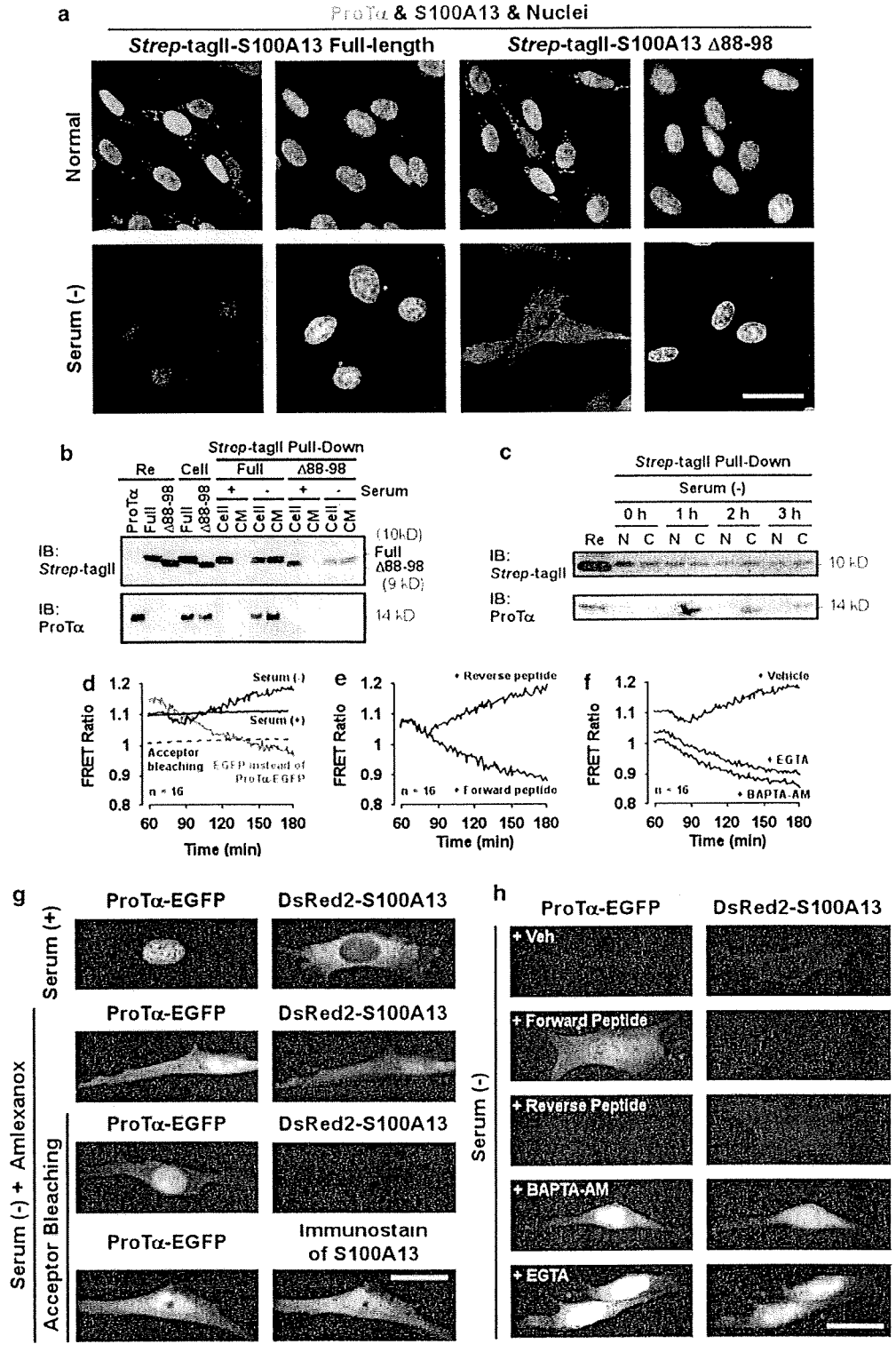




NPG.CDD.CDD201052

release.[8] S100A13 has two EF-hand $Ca^{2+}$-binding motifs and belongs to a member of the S100 family.[15–17] It has been reported that S100A13 is involved in the non-classical extracellular release of target molecules containing fibroblast growth factor-1 (FGF-1) and interleukin-1α.[9–11,19,34,35] In this study, we successfully showed that ProTα is another example of stress-induced non-vesicular extracellular release, using S100A13, a cargo molecule. Furthermore, we revealed that the C-terminal regions of ProTα and S100A13 are essential for their interaction, which precedes extracellular release of both proteins, and that caspase-3 cleaves off C-terminal regions of ProTα. Thus, the non-vesicular extracellular release of ProTα has a unique feature that it is does not occur under the condition of apoptosis.

The unique point in this study is observed in the fact that ProTα is strictly localized in the nucleus in neurons, astrocytes, and C6 glioma cells. The mechanism underlying ischemic stress-induced extracellular release of ProTα comprises a two-tier export system: from the nucleus to the cytosol, and from the cytosol to outside the cell. As mentioned above, the nuclear export of ProTα is attributed to ischemia-induced ATP loss, which impairs the importin-NLS mechanism. As this nuclear export was not affected by leptomycin B, the serum-deprivation stress-induced drastic decrease in nuclear levels of ProTα is likely to be due to passive diffusion. Interestingly, once ProTα is exported from the nucleus, it is disappeared without remaining in the cytosol. In other words, nuclear export is the rate-limiting step for non-vesicular and extracellular release of ProTα.

The stress-induced extracellular release of ProTα was impaired by the addition of cytosolic or extracellular $Ca^{2+}$-chelating agents. The interaction between ProTα and S100A13 was $Ca^{2+}$ concentration dependent in the range 0.1–200 μM, which corresponds to the cellular levels between resting and stimulated conditions. The $Ca^{2+}$ dependency seems to be attributed to the facts that both S100A13 and ProTα are $Ca^{2+}$-binding proteins.[15–17,36] On the basis of the observation that serum-deprivation stress causes the activation of voltage-dependent N-type $Ca^{2+}$ channel, which is involved in the non-classical release of FGF-1 and S100A13,[34,35] ischemic stress-induced $Ca^{2+}$ influx may underlie the non-vesicular ProTα release as the second step after ATP loss-dependent nuclear release.

Neurons die by necrosis in the low density of culture under the serum-starved condition, but their survival activity increases as the cell density goes. We identified ProTα as the important molecule, which is released in the CM of serum-starved culture of neurons, and suppresses the necrosis through a recovery of glucose transport and ATP supply.[5,37] After longer culture with ProTα, however, we found that neurons die by apoptosis through activation of caspase-3.[5] As caspase-3 is known to cleave poly-[ADP-ribose] polymerase, which consumes abundant ATP molecule for the restoration from stress-induced damage of DNA,[38] this machinery seems to have some functions in suppression of rapid necrosis by stress.[29] As the concomitant addition of anti-apoptotic neurotrphins with ProTα completely inhibits the cell death, the physiological meaning of ProTα action would be speculated as a conversion of uncontrollable cell death necrosis to controllable apoptosis. Indeed, this speculation was confirmed by *in vivo* study, in which exogenous ProTα inhibited both necrosis and apoptosis of retinal cells after ischemia, but the further treatment with anti-BDNF antibody disclosed the apoptosis induction by ProTα.[7]

It should be noted that ProTα in the cytosol inhibits apoptosis through an inhibition of apoptosome formation in non-neuronal HeLa cells.[4] Furthermore, there is a report that ProTα is released from the nuclei when the NLS is cleaved off by caspase-3.[20,21] This study clearly showed that the C-terminal region of ProTα including NLS is cleaved in culture by the apoptosis-induced compound, and in cell-free digestion of recombinant ProTα by active caspase-3 (Figure 6d–g). As ProTα devoid of C-terminal region (a.a.98 or 99–112) is conceived to lose the activity of interaction with S100A13 (Figure 4d), it will remain in the cytosol without extracellular release. All these findings enable us to speculate that ProTα extracellularly released on the necrosis condition inhibits neuronal necrosis in an autocrine or paracrine manner, whereas cytosolic ProTα redistributed from the nuclei on the apoptotic condition may have an anti-apoptotic self-defensive function.

It is well known that several endogenous molecules are released in response to injury, infection, or other inflammatory stimuli, and initiate inflammatory responses. These molecules are so-called damage-associated molecular patterns (DAMPs) and/or alarmins.[39,40] Although DAMPs have

**Figure 5** S100A13 is a cargo molecule mediating extracellular ProTα release. (**a**) S100A13 Δ88–98 mutant as a dominant-negative regulator of ProTα release. Distributions of ProTα and *Strep*-tagII-S100A13 mutants in cultured C6 glioma cells with or without serum. (**b**) Loss of interaction of the *Strep*-tagII-S100A13 Δ88–98 mutant with ProTα in living cells. Cells and CM from C6 glioma cells stably expressing *Strep*-tagII-S100A13 mutants with or without serum (3 h) were harvested and a *Strep*-tagII pull-down assay was performed. Re: recombinant rat proteins. (**c**) The interaction of the *Strep*-tagII-S100A13 with ProTα occurs in cytosol, but not nucleus. Nucleus (N) and cytosol (C) from C6 glioma cells stably expressing *Strep*-tagII-S100A13 mutants with or without serum (3 h) were prepared and a *Strep*-tagII pull-down assay was performed. (**d–f**) Imaging of the ProTα–S100A13 interaction in living cells. Time-course of FRET images after serum-deprivation stress in phenol red-free DMEM. DsRed2-S100A13 was transiently expressed in C6 glioma cells stably expressing ProTα-EGFP. The FRET ratio represents the emission ratio of 590/520 nm. (**d**) Serum-deprivation stress-induced increase in the FRET emission ratio. Cell population images of FRET were measured in the presence of amlexanox (100 μM). Serum-deprivation stress caused an increase in the emission ratio from approximately 90 min. When the acceptor (DsRed2-S100A13) was earlier bleached, serum-deprivation stress did not increase the emission ratio. In cells expressing EGFP instead of ProTα-EGFP, FRET did not occur after serum deprivation. (**e**) Inhibition of FRET by the ProTα C-terminal peptide. Cellular delivery of a C-terminal peptide (amino-acids 102–112; forward peptide) of ProTα abolished increase of FRET emission ratio and decreased basal level, whereas no change was observed with the reverse peptide. (**f**) Inhibition of FRET by $Ca^{2+}$ chelating. Cytosolic and extracellular $Ca^{2+}$-chelating agents, BAPTA-AM, and EGTA, respectively, inhibited FRET after serum deprivation. A decrease in the basal level of the emission ratio was observed approximately 70 min after the stress, suggesting that nuclear ProTα-EGFP is redistributed into the cytosol, but does not interact with S100A13 in the absence of $Ca^{2+}$. BAPTA-AM and EGTA were used at 1 μM and 1 mM, respectively. (**g**) Subcellular distribution of ProTα-EGFP and DsRed2-S100A13. The images were collected 180 min after serum deprivation after FRET analysis. (**h**) Inhibition of extracellular release of ProTα-EGFP and DsRed2-S100A13. The images were collected 180 min after serum-deprivation stress. Scale bars represent 20 μm



NPG.CDD.CDD201052

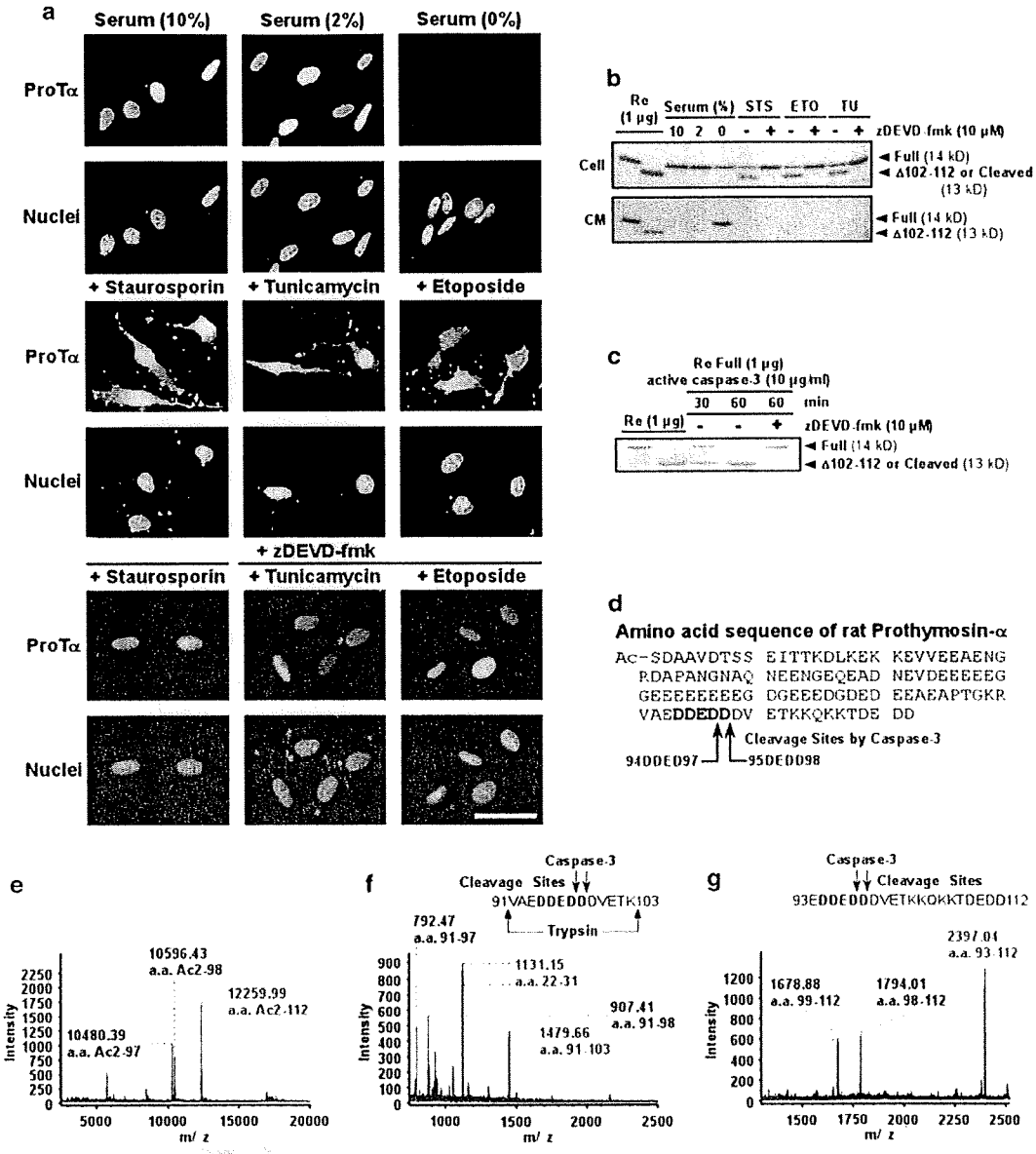


**Figure 6** Apoptotic stress induces re-distribution of ProTα. **(a)** Altered distribution of ProTα in C6 glioma cells. Cells were subjected to serum-reduced (2%) or serum-deprivation stress for 3 h. Cells were treated with staurosporine, tunicamycin, or etoposide for 3 h in the presence or absence of zDEVD-fmk (10 μM). All apoptogenic compounds were used at 1 μM in 2% serum-containing medium. Scale bars represent 20 μm. **(b)** Cleavage, but not release of ProTα by apoptogenic compounds treatment. STS, staurosporine; TU, tunicamycin; ETO, etoposide. **(c)** Rat ProTα as a caspase-3 substrate. Recombinant (Re) rat ProTα (1 μg) was incubated with 10 μg/ml recombinant active caspase-3 in the presence or absence of 10 μM zDEVD-fmk for 1 h at 37°C. Recombinant rat ProTα Δ102–112 mutant was used as a marker of ProTα fragment lacking the C-terminal region. **(d)** Cleavage sites of rat ProTα by active caspase-3. **(e–g)** Identification of cleavage sites of rat ProTα by active caspase-3 by use of MALDI-TOF analysis. **(e)** Generation of two truncated types of ProTα by apoptogenic compound treatment. Peaks of intracellular native ProTα and cleaved ProTα by staurosporine treatment were shown as blue and black, respectively. The molecular mass of 12259.99 represents N-terminal serine acetylated full-length size (Ac2-112). The molecular mass of 10480.39 or 10596.43, which corresponds to C-terminal truncated ProTα Ac2-97 or Ac2-98, respectively. **(f)** Characterization of cleavage of ProTα by caspase-3 by peptide mass fingerprinting. Recombinant rat ProTα was incubated with or without active rat caspase-3, followed by a separation with SDS-PAGE, in-gel digestion of protein bands with trypsin and MALDI-TOF analysis. In the absence of incubation of active rat capase-3 (blue peaks), two peaks with molecular mass of 1131.15 and 1479.66 were identified as a.a.22–31 and a.a.91–103 peptides, respectively. However, in its presence (black peaks), there were new peaks with 792.47 and 907.41, corresponding to a.a.91–97 and a.a.91–98 peptides, respectively, but the peak with 1479.66 disappeared. **(g)** Cleavage of rat ProTα C-terminal regions by active caspase-3. Blue peak with molecular mass of 2397.04 represents synthetic rat ProTα C-terminal 93–112 polypeptide. The digestion of C-terminal polypeptide by caspase-3 produced two peaks with molecular mass of 1678.88 and 1794.01, which correspond to a.a.99–112 and a.a.98–112 peptides, respectively

intranuclear and/or intracellular functions under normal conditions, they have extracellular effects under pathological conditions. High-mobility group box1 (HMGB1), a representative DAMP molecule, has similar characteristics to ProTα. HMGB1, a nuclear protein, is released by necrotic stress, but not by apoptosis, as seen for ProTα. However, it causes



NPG.CDD.CDD201052

cell damaging or inflammatory actions. Although this release is reported to occur through passive diffusion through necrosis-induced membrane disruption, detailed characterization of the mechanism is required. It is interesting to propose that ProTα is a novel type of DAMP bearing cell-defensive functions in brain.

In conclusion, we showed that the nuclear protein ProTα is extracellularly released from neurons, astrocytes, and C6 glioma cells on ischemic stress in a non-vesicular manner. The initial step of this release is nuclear release of ProTα owing to the stress-induced ATP loss. Non-vesicular extracellular release of ProTα is dependent on a $Ca^{2+}$-sensitive interaction with S100A13. We also showed that ProTα loses the ability to undergo extracellular release under apoptotic conditions, owing to loss of its interaction with S100A13, a cargo molecule.

## Materials and Methods

**Materials and antibodies.** Brefeldin A was purchased from Nacalai Tesque (Kyoto, Japan). The 2-DG, staurosporine, tunicamycin, etoposide, and leptomycin B were purchased from SIGMA (St. Louis, MO, USA). Wheat germ agglutinin was purchased from Biomeda Corp. (Burlingame, CA, USA). Amlexanox was kindly provided by Takeda Pharmaceutical Company Ltd. (Osaka, Japan). Rat ProTα C-terminal synthetic peptides (amino-acids 102–112: forward sequence, TKKQKKTDEDD; reverse sequence, DDEDTKKQKKT; amino-acids 93–112: forward sequence, EDDEDDDVETKKQKKTDEDD) were purchased from Bio Synthesis Inc. (Lewisville, TX, USA). Mouse anti-ProTα antibody was kindly provided by Dr. AB Vartapetian (Moscow State University, Moscow, Russia) or purchased from Alexis Biochemicals (Lausen, Switzerland). These two antibodies are derived from the same source. Goat anti-importin α1 and normal goat antibody were purchased from Santa Cruz Biotechnology Inc. (Santa Cruz, CA, USA) and ICN/Cappel Inc. (Durham, NC, USA), respectively. Rabbit anti-S100A13 antibody was kindly provided by Dr. T Maciag (Center for Molecular Medicine, Maine Medical Center Research Institute, Scarborough, ME, USA).

**Expression constructs and purification procedures for proteins.** The rat ProTα gene was amplified from cDNA derived from rat embryonic brain. The PCR primers used were ProTα-F, 5′-AACATATGTCAGACGCGGCAGTGGA-3′ (containing a NdeI site), and ProTα-R, 5′-AAGGATCCAGTGGAGGGTGAATAGGTCAC-3′ (containing a BamHI site). Recombinant ProTα protein was constructed by cloning the amplified ProTα gene in-frame into the NdeI-BamHI sites of pET-20b (Novagen, San Diego, CA, USA). Native and recombinant ProTα were purified using a phenol extraction procedure[41] and visualized with Coomassie Brilliant Blue (Gelcode blue stain reagent: PIERCE Biotechnology, Rockford, IL, USA). Recombinant GST-ProTα deletion mutants were constructed by cloning the amplified genes blunted at their 5′-ends and cloned in-frame into the BamHI (blunted)-EcoRI sites of pGEX-5X-1 (GE Healthcare Bio-Science Corp., Piscataway, NJ, USA). The PCR primers used were as follows: Full-F, 5′-AGGGATCCAATGTCAGACGCGGCAGAG-3′; Δ1–68-F, 5′-AGGGATCCAATGGAAGGTGATGGTGAGGAAG-3′; Δ1–86-F, 5′-AGGGATCCAATGACGGGCAAGCGGGTAGCTG-3′; Full-R, 5′-TTGAATTCCTAGTCATCCTCATCAGTCTTC-3′; Δ79–112-R, 5′-TTGAATTCCTAATCTCCATCTTCTTCCTC-3′; and Δ102–112-R, 5′-TTGAATTCCTACTCAACATCATCATCCTCATC-3′. All F-primers contain a BamHI site, whereas all R-primers contain a stop codon and an EcoRI site. The recombinant proteins were purified using Glutathione-Sepharose (GE Healthcare Bio-Science Corp.). An EGFP-ProTα fusion protein, for mammalian expression, was constructed by cloning the amplified genes in-frame into the SacI-SalI sites of pEGFP-N3 (BD Bioscience Clontech, Palo Alto, CA, USA). The PCR primers used were ProTα-F2, 5′-AAGAGCTCATGTCAGACGCGGCAGTGGA-3′ (containing a SacI site), and ProTα-R2, 5′-AAGTCGACGTCATCCTCATCAGTCTTCT-3′ (containing a SalI site). Plasmid construction and purification procedure of recombinant *Strep*-tagII-S100A13 protein (full length and Δ88–98) were performed as described earlier.[34] DsRed2-S100A13 fusion protein, for mammalian expression, was constructed by cloning. The rat S100A13 gene was amplified from cDNA derived from rat embryonic brain. The PCR primers used were S100A13-F, 5′-AAGAATTCATGGCAGCAGAGCCCCCGAC-3′, and S100A13-R, 5′-AAAAGCTTTTACTTCTTGCGAATCGCCAGG-3′. The amplified S100A13 gene was cloned into pGEM-T Easy (Promega, Tokyo, Japan), and sub-cloned in-frame into the NotI-SpeI sites of pBluescript SK (Stratagene, La Jolla, CA, USA). Finally, the S100A13 gene was sub-cloned in-frame into the SacI-BamHI sites of pDsRed2-C1 (BD Bioscience Clontech). After cloning, each construct was verified by sequencing. The *Escherichia coli* strains DH10B and BL21 (DE3) were transformed with each of these constructs for sub-cloning and protein expression, respectively. For the analysis of protein–protein interactions and their modulation by ions, we adopted the following molecular weight values (average mass) for full-length GST-ProTα and *Strep*-tagII-S100A13, Ca, and Cu: 39 016.19, 13 840.08, 40.078, and 63.546, respectively.

**Cell culture, gene transfection, and peptide delivery.** Primary cultures of neurons and astrocytes from 17-day-old embryonic rat brain, and cultures of C6 glioma cells, were prepared as described earlier.[34,42] Gene constructs were transfected with the NeuroPORTER reagent (Gene Therapy Systems, Inc., San Diego, CA, USA). C6 glioma cells stably expressing recombinant protein were selected and maintained in 1 mg/ml G418. Recombinant protein expression was confirmed in isolated clones by microscopy and by immunoblotting. Synthetic peptides were delivered into living cells using the BioPORTER protein delivery reagent (Gene Therapy Systems, Inc.).

**Immunocytochemistry.** Cells were fixed in 4% paraformaldehyde in PBS for 30 min and then permeabilized with methanol for 10 min at room temperature. The fixed cells were washed with PBS, incubated in blocking buffer (1% BSA and 0.1% Triton X-100 in PBS) for 3 h at 4°C, and then incubated in primary antibody (1 : 300 dilution in blocking buffer) overnight at 4°C. Next, the cells were incubated in a secondary antibody conjugated to FITC or Cy3 (Chemicon International Inc., Temecula, CA, USA), and then with rhodamine-conjugated streptavidin (Chemicon International Inc.), each diluted 1 : 500 in blocking buffer. The nuclei were visualized with Hoechst 33342 or propidium iodide (Molecular Probes, Eugene, OR, USA). Images were collected using a BZ-8000 microscope (KEYENCE, Osaka, Japan) with a ×20 Plan APO lens (Nikon, Tokyo, Japan) or using an LSM 510 META confocal laser microscope with a ×40 Plan-Neofluar lens or a ×63 Plan-Apochromat lens (Carl Zeiss, Oberkochen, Germany).

**Gravimetric measurements with a biosensor QCM.** Protein–protein interactions were detected using an AffinixQ system (Initium Inc., Tokyo, Japan), a QCM sensor device. Detailed procedures have been described earlier.[19] AT-cut quartz crystals coated with a thin gold surface layer with a fundamental frequency of 27 MHz were used. Immediately before use, the gold surface of the quartz resonator was cleaned with piranha solution ($H_2SO_4$: 30% $H_2O_2 = 3:1$) for 5 min, and thoroughly washed with double-distilled water. An anti-GST antibody (GE Healthcare Bio-Sciences Corp.) or a streptavidin-conjugated antibody solution (ICN/Cappel Inc.) was applied to the resonator for 30 min to obtain a layer for immobilization of GST-ProTα or *Strep*-tagII-S100A13, respectively. Next, the resonator was rinsed with interaction buffer (50 mM Tris–HCl pH 7.6, 15 mM NaCl, 140 mM KCl), immersed in interaction buffer (8 ml), and then subjected to immobilization of GST-ProTα or *Strep*-tagII-S100A13 for 30 min before being placed in fresh interaction buffer. The protein–protein interactions were determined from the frequency changes (OU: $\Delta F$ in Hz) owing to changes in the mass on the electrode at the sub-nanogram level, on application of a small volume (1–10 μl) of protein solution. On the basis of the Sauerbrey formula, an increase of 1 Hz OU is calculated as an interaction of 30.38 pg of a molecule with the biosensor. In all immobilizations of GST-ProTα on the resonator, it was confirmed that approximately 430 fmol of GST-ProTα was immobilized as an absolute amount (an increase of OU: 550 Hz). All experiments were carried out at 25 ± 1 °C. All sensorgram data show the OU value after the association phase. For kinetic analysis, frequency changes induced by cumulatively applied protein were curve fitted to the formula $\Delta F = A(e^{(-1/\tau)T} - 1)$, and the $1/\tau$ value was plotted for each concentration of added protein. $1/\tau$ and $K_D$ represent $k_a[X] + k_d$ and $k_d/k_a$, respectively, where X is the concentration of the added protein. $K_D$, $k_a$, and $k_d$ denote dissociation constant, association rate constant, and dissociation rate constant, respectively.

**Co-immunoprecipitation analysis and *Strep*-tagII pull-down assay.** For the determination of protein release, cell lysis buffer (150 mM NaCl, 1 μM $CaCl_2$, 50 mM Tris–HCl pH 7.8, 1% Triton X-100, and protease inhibitor cocktail) was added to cells ($0.5–2 \times 10^6$ cells) to a final volume of 1 ml and the samples were sonicated. Cells and CM (1 ml) samples were used after the removal



NPG.CDD.CDD201052

of insoluble debris by centrifugation at 10 000 × *g*. For immunoprecipitation analysis, anti-ProTα or pre-immune antibodies and protein G-Sepharose beads (GE Healthcare Bio-Science Corp.) were added to CM and incubated on a rotor for 2 h at 4 °C. For preparation of nuclear and cytosolic fractions, cells were harvested by cell lysis buffer and then homogenized by dounce homogenizer. Nuclear fraction was collected by centrifugation at 1000 × *g* and supernatant fluid was used as cytosolic fraction. For the *Strep*-tagII pull-down assay, StrepTactin-Sepharose beads were added to cells or CM samples and incubated on a rotor for a further 1 h at 4 °C. The beads were washed three times with lysis buffer and quenched with 50 μl of SDS sample buffer.

**Immunoblotting for ProTα (acidic blotting).** Samples obtained by boiling cultured cells for 5 min or samples of recombinant ProTα in Laemmli sample buffer were subjected to 15% SDS-PAGE fractionation and electrotransferred onto nitrocellulose membranes in acidic conditions in 20 mM sodium acetate buffer, pH 5.2, followed by fixation with 0.5% glutaraldehyde.[14] The membranes were blocked with 5% non-fat milk in TBST (20 mM Tris–HCl, pH 7.6, 150 mM NaCl, 0.1% Tween-20) and probed with the antibody against ProTα (1 μg/ml in 1% non-fat milk/TBST). Detection was performed using an HRP-conjugated goat anti-mouse IgG (Zymed Laboratories, San Francisco, CA, USA) and SuperSignal West Pico Chemiluminescent Substrate (PIERCE Biotechnology).

**ATP measurement assay.** Intracellular ATP was extracted from cells in the exponential phase of growth and measured by the luciferin/luciferase method using an ATP-Determination kit (Molecular Probes). Samples containing a total of $2 \times 10^6$ cells were subjected to the assay. Reaction buffer (200 μl) containing 0.5 μM luciferin, 1.25 μg/ml luciferase, and 1 mM DTT was mixed with each cell lysate (20 μl), and the luminescence was analyzed using a LUMAT LB 9507 luminometer (EG&G Berthold, Bad Wildbad, Germany).

**Microinjection and time-lapse photography.** C6 glioma cells were grown at a density of $2 \times 10^5$ cells/cm$^2$ on glass-bottom 35-mm dishes (Matsunami Glass Industries Ltd., Osaka, Japan) for 24 h at 37°C before use in experiments. The cells were imaged in Hanks buffer with or without serum. Microinjection was performed using an InjectMan NI2 microinjection system (Eppendorf AG, Hamburg, Germany). ProTα and BSA were conjugated to Alexa Fluor488 and with Alexa Fluor568 (Molecular Probes), respectively. Fluorescently labeled proteins (10 μM in a needle) or ATP (3 mM in a needle) were injected into a cell at 45 hPa for 0.2 s. The injected fluorescently labeled proteins and fluorescent protein-fusion recombinants were imaged using an Axiovert 200 inverted microscope (Carl Zeiss) with a × 40 Plan-Neofluar lens or a × 63 Plan-Apochromat lens.

**Fluorescence resonance energy transfer.** C6 glioma cells expressing ProTα-EGFP and DsRed2-S100A13 were plated onto 96-well glass microplates and imaged in phenol red-free DMEM at 37°C. The fluorescence in each well was analyzed using a Fluostar Optima microplate reader (BMG Labtechnologies, Offenburg, Germany) with a 10-nm bandwidth excitation filter at 485 nm, and 10-nm bandwidth emission filters corresponding to 520 and 590 nm filters. The gain settings were identical for all experiments to maintain the relative contributions of the fluorescence to the detection channels contrast for spectral un-mixing. The 590/520-nm ratiometric images were acquired every 1 min for 120 min. The FRET efficiency was calculated as direct sensitization of the acceptor corresponding to acceptor fluorescence after excitation at 544 nm (acceptor photo-bleaching).

***In vitro* cleavage assay by caspase-3.** Recombinant rat ProTα (1 μg) was incubated with 10 μg/ml recombinant active caspase-3 (Chemicon International Inc.) in the presence or absence of 10 μM zDEVD-fmk (BD Biosciences, San Jose, CA, USA), a specific caspase group II inhibitor, in caspase buffer (20 mM PIPES pH 7.4, 100 mM NaCl, 1 mM EDTA, 0.1% CHAPS, 10% sucrose, and 10 mM DTT) for 1 h at 37°C.

**Matrix-assisted laser desorption/ionization-time of flight.** S100A13 was identified by using one-dimensional electrophoresis with in-gel digestion of bands followed by MALDI-TOF using an Ultraflex TOF/TOF system (Bruker Daltonics Inc., Billerica, MA, USA). Cleavage sites of rat ProTα by active caspase-3 were also identified by MALDI-TOF analysis. Detailed procedures have been described earlier.[34]

**Statistical analysis.** All results are shown as means ± S.E.M. Two independent groups were compared using the Student's *t*-test. Multiple groups were compared using Dunnett's multiple comparison test after a one-factor ANOVA. $P<0.05$ was considered significant.

## Conflict of interest

The authors declare no conflict of interest.

**Acknowledgements.** We thank K Kidera, N Kiguchi, and N Takayama for technical assistance, and A Yoshida for valuable suggestions. We acknowledge Takeda Pharmaceutical Company Ltd., AB Vartapetian, and T. Maciag for providing amlexanox, the mouse anti-ProTα antibody, and the rabbit anti-S100A13 antibody. Parts of this study were supported by Grants-in-Aid for Scientific Research (to HU, B: 13470490 and B: 15390028) and Young Scientists (to HM, B: 20770105), on Priority Areas – Research on Pathomechanisms of Brain Disorders (to HU, 17025031, 18023028, 20023022) from the Ministry of Education, Culture, Sports, Science and Technology (MEXT), the Japan Society for the Promotion of Science (JSPS), and Health and Labour Sciences Research Grants on Research on Biological Resources and Animal Models for Drug Development (to HU, H20-Research on Biological Resources and Animal Models for Drug Development-003) from the Ministry of Health, Labour and Welfare.

1. Piñeiro A, Cordero OJ, Nogueira M. Fifteen years of prothymosin alpha: contradictory past and new horizons. *Peptides* 2000; **21**: 1433–1446.
2. Letsas KP, Frangou-Lazaridis M. Surfing on prothymosin alpha proliferation and anti-apoptotic properties. *Neoplasma* 2006; **53**: 92–96.
3. Gómez-Márquez J. Function of prothymosin alpha in chromatin decondensation and expression of thymosin beta-4 linked to angiogenesis and synaptic plasticity. *Ann N Y Acad Sci* 2007; **1112**: 201–209.
4. Jiang X, Kim HE, Shu H, Zhao Y, Zhang H, Kofron J *et al.* Distinctive roles of PHAP proteins and prothymosin-alpha in a death regulatory pathway. *Science* 2003; **299**: 223–226.
5. Ueda H, Fujita R, Yoshida A, Matsunaga H, Ueda M. Identification of prothymosin-alpha1, the necrosis-apoptosis switch molecule in cortical neuronal cultures. *J Cell Biol* 2007; **176**: 853–862.
6. Fujita R, Ueda H. Prothymosin-alpha1 prevents necrosis and apoptosis following stroke. *Cell Death Differ* 2007; **14**: 1839–1842.
7. Fujita R, Ueda M, Fujiwara K, Ueda H. Prothymosin-alpha plays a defensive role in retinal ischemia through necrosis and apoptosis inhibition. *Cell Death Differ* 2009; **16**: 349–358.
8. Prudovsky I, Mandinova A, Soldi R, Bagala C, Graziani I, Landriscina M *et al.* The non-classical export routes: FGF1 and IL-1alpha point the way. *J Cell Sci* 2003; **116**: 4871–4881.
9. Mouta Carreira C, LaVallee TM, Tarantini F, Jackson A, Lathrop JT, Hampton B *et al.* S100A13 is involved in the regulation of fibroblast growth factor-1 and p40 synaptotagmin-1 release *in vitro*. *J Biol Chem* 1998; **273**: 22224–22231.
10. Landriscina M, Soldi R, Bagalá C, Micucci I, Bellum S, Tarantini F *et al.* S100A13 participates in the release of fibroblast growth factor 1 in response to heat shock *in vitro*. *J Biol Chem* 2001; **276**: 22544–22552.
11. Mandinova A, Soldi R, Graziani I, Bagala C, Bellum S, Landriscina M *et al.* S100A13 mediates the copper-dependent stress-induced release of IL-1alpha from both human U937 and murine NIH 3T3 cells. *J Cell Sci* 2003; **116**: 2687–2696.
12. Yasuda Y, Miyamoto Y, Saiwaki T, Yoneda Y. Mechanism of the stress-induced collapse of the Ran distribution. *Exp Cell Res* 2006; **312**: 512–520.
13. Shakulov VR, Vorobjev IA, Rubtsov YP, Chichkova NV, Vartapetian AB. Interaction of yeast importin alpha with the NLS of prothymosin alpha is insufficient to trigger nuclear uptake of cargos. *Biochem Biophys Res Commun* 2000; **274**: 548–552.
14. Sukhacheva EA, Evstafieva AG, Fateeva TV, Shakulov VR, Efimova NA, Karapetian RN *et al.* Sensing prothymosin alpha origin, mutations and conformation with monoclonal antibodies. *J Immunol Methods* 2002; **266**: 185–196.
15. Heizmann CW, Fritz G, Schäfer BW. S100 proteins: structure, functions and pathology. *Front Biosci* 2002; **7**: d1356–d1368.
16. Zimmer DB, Wright Sadosky P, Weber DJ. Molecular mechanisms of S100-target protein interactions. *Microsc Res Tech* 2003; **60**: 552–559.
17. Imai FL, Nagata K, Yonezawa N, Nakano M, Tanokura M. Structure of calcium-bound human S100A13 at pH 7.5 at 1.8 A resolution. *Acta Crystallogr Sect F Struct Biol Cryst Commun* 2008; **64**: 70–76.
18. Shishibori T, Oyama Y, Matsushita O, Yamashita K, Furuichi H, Okabe A *et al.* Three distinct anti-allergic drugs, amlexanox, cromolyn and tranilast, bind to S100A12 and S100A13 of the S100 protein family. *Biochem J* 1999; **338** (Part 3): 583–589.
19. Matsunaga H, Ueda H. Synergistic $Ca^{2+}$ and $Cu^{2+}$ requirements of the FGF1-S100A13 interaction measured by quartz crystal microbalance: an initial step in amlexanox-reversible non-classical release of FGF1. *Neurochem Int* 2008; **52**: 1076–1085.



NPG.CDD.CDD201052

20. Enkemann SA, Wang RH, Trumbore MW, Berger SL. Functional discontinuities in prothymosin alpha caused by caspase cleavage in apoptotic cells. *J Cell Physiol* 2000; **182**: 256–268.
21. Evstafieva AG, Belov GA, Rubtsov YP, Kalkum M, Joseph B, Chichkova NV *et al.* Apoptosis-related fragmentation, translocation, and properties of human prothymosin alpha. *Exp Cell Res* 2003; **284**: 211–223.
22. Karetsou Z, Martic G, Tavoulari S, Christoforidis S, Wilm M, Gruss C *et al.* Prothymosin alpha associates with the oncoprotein SET and is involved in chromatin decondensation. *FEBS Lett* 2004; **577**: 496–500.
23. Subramanian C, Hasan S, Rowe M, Hottiger M, Orre R, Robertson ES. Epstein-Barr virus nuclear antigen 3C and prothymosin alpha interact with the p300 transcriptional coactivator at the CH1 and CH3/HAT domains and cooperate in regulation of transcription and histone acetylation. *J Virol* 2002; **76**: 4699–4708.
24. Karetsou Z, Kretsovali A, Murphy C, Tsolas O, Papamarcaki T. Prothymosin alpha interacts with the CREB-binding protein and potentiates transcription. *EMBO Rep* 2002; **3**: 361–366.
25. Martini PG, Katzenellenbogen BS. Modulation of estrogen receptor activity by selective coregulators. *J Steroid Biochem Mol Biol* 2003; **85**: 117–122.
26. Karapetian RN, Evstafieva AG, Abaeva IS, Chichkova NV, Filonov GS, Rubtsov YP *et al.* Nuclear oncoprotein prothymosin alpha is a partner of Keap1: implications for expression of oxidative stress-protecting genes. *Mol Cell Biol* 2005; **25**: 1089–1099.
27. Ueda H, Fujita R. Cell death mode switch from necrosis to apoptosis in brain. *Biol Pharm Bull* 2004; **27**: 950–955.
28. Ueda H. Prothymosin alpha plays a key role in cell death mode-switch, a new concept for neuroprotective mechanisms in stroke. *Naunyn Schmiedebergs Arch Pharmacol* 2008; **377**: 315–323.
29. Ueda H. Prothymosin alpha and cell death mode switch, a novel target for the prevention of cerebral ischemia-induced damage. *Pharmacol Ther* 2009; **123**: 323–333.
30. Jahn R, Scheller RH. SNAREs—engines for membrane fusion. *Nat Rev Mol Cell Biol* 2006; **7**: 631–643.
31. Martens S, McMahon HT. Mechanisms of membrane fusion: disparate players and common principles. *Nat Rev Mol Cell Biol* 2008; **9**: 543–556.
32. Nickel W. The mystery of nonclassical protein secretion. A current view on cargo proteins and potential export routes. *Eur J Biochem* 2003; **270**: 2109–2119.
33. Nickel W, Rabouille C. Mechanisms of regulated unconventional protein secretion. *Nat Rev Mol Cell Biol* 2009; **10**: 148–155.
34. Matsunaga H, Ueda H. Evidence for serum-deprivation-induced co-release of FGF-1 and S100A13 from astrocytes. *Neurochem Int* 2006; **49**: 294–303.
35. Matsunaga H, Ueda H. Voltage-dependent N-type $Ca^{2+}$ channel activity regulates the interaction between FGF-1 and S100A13 for stress-induced non-vesicular release. *Cell Mol Neurobiol* 2006; **26**: 237–246.
36. Chichkova NV, Evstafieva AG, Lyakhov IG, Tsvetkov AS, Smirnova TA, Karapetian RN *et al.* Divalent metal cation binding properties of human prothymosin alpha. *Eur J Biochem* 2000; **267**: 4745–4752.
37. Fujita R, Ueda H. Protein kinase C-mediated necrosis-apoptosis switch of cortical neurons by conditioned medium factors secreted under the serum-free stress. *Cell Death Differ* 2003; **10**: 782–790.
38. Decker P, Muller S. Modulating poly (ADP-ribose) polymerase activity: potential for the prevention and therapy of pathogenic situations involving DNA damage and oxidative stress. *Curr Pharm Biotechnol* 2002; **3**: 275–283.
39. Lotze MT, Tracey KJ. High-mobility group box 1 protein (HMGB1): nuclear weapon in the immune arsenal. *Nat Rev Immunol* 2005; **5**: 331–342.
40. Harris HE, Raucci A. Alarmin(g) news about danger: workshop on innate danger signals and HMGB1. *EMBO Rep* 2006; **7**: 774–778.
41. Sburlati AR, Manrow RE, Berger SL. Human prothymosin alpha: purification of a highly acidic nuclear protein by means of a phenol extraction. *Protein Expr Purif* 1990; **1**: 184–190.
42. Fujita R, Ueda H. Protein kinase C-mediated cell death mode switch induced by high glucose. *Cell Death Differ* 2003; **10**: 1336–1347.

Supplementary Information accompanies the paper on Cell Death and Differentiation website (http://www.nature.com/cdd)



NPG.CDD.CDD201052

Pharmacology & Therapeutics 123 (2009) 323–333

Contents lists available at ScienceDirect

Pharmacology & Therapeutics

journal homepage: www.elsevier.com/locate/pharmthera

Associate editor: M. Endoh

# Prothymosin α and cell death mode switch, a novel target for the prevention of cerebral ischemia-induced damage

Hiroshi Ueda *

*Division of Molecular Pharmacology and Neuroscience, Nagasaki University Graduate School of Biomedical Sciences, 1-14 Bunkyo-machi, Nagasaki 852-8521, Japan*

ARTICLE INFO

*Keywords:*
Necrosis
Apoptosis
Glucose transporter
Glia
Protein kinase C
Brain-derived neurotrophic factor

ABSTRACT

Following stroke or traumatic damage, neuronal death via both necrosis and apoptosis causes loss of functions including memory, sensory perception and motor skills. Since necrosis has the nature to expand, while apoptosis stops the cell death cascade in the brain, necrosis is considered to be a promising target for rapid treatment for stroke. Pure neuronal necrosis occurs when cortical neurons are cultured under serum-free and low-density conditions. Prothymosin α (ProTα) isolated from conditioned medium after serum-free culture was found to prevent necrosis by recovering the energy crisis due to endocytosed glucose transporters. At a later time point under the same starvation conditions, ProTα causes apoptosis, which in turn seems to inhibit the rapidly occurring necrosis by cleaving poly (ADP-ribose) polymerase, a major machinery involved in ATP consumption. Indeed, ProTα administered via systemic routes markedly inhibits the histological and functional damage induced by cerebral and retinal ischemia. Although ProTα also causes a cell death mode switch from necrosis to apoptosis in vivo, the induced apoptosis was found to be completely inhibited by endogenously occurring brain-derived neurotrophic factor or erythropoietin. Since forced downregulation of ProTα deteriorates the ischemic damage, it is evident that ProTα plays in vivo neuroprotective roles after ischemic events. Analyses in terms of the therapeutic time window and potency suggest that ProTα could be the prototypic compound to develop the medicine useful for treatment of stroke in clinics.



**Contents**



*Abbreviations:* AS-ODN, antisense oligodeoxynucleotide; BCCAO, Bilateral common carotid artery occlusion; BDNF, brain-derived neurotrophic factor; caspases, cysteinyl aspartate-specific proteases; 2-DG, 2-deoxyglucose; EPO, erythropoietin; ER, endoplasmic reticulum; ERG, electroretinography; GCL, the ganglion cell layer; GLUT, glucose transporter; INL, inner nuclear layer; LOG, low-oxygen and low-glucose; MALDI-TOF MS, matrix-assisted laser desorption/ionization-time of flight mass spectrometry; MCAO, middle cerebral artery occlusion; mPTP, mitochondrial permeability transition pore; NLS, nuclear localization signal; ONL, outer nuclear layer; PARP, poly (ADP-ribose) polymerase; PI, propidium iodide; PKC, protein kinase C; PLA2, phospholipase A2; PLC, phospholipase C; ProTα, Prothymosin α; ROS, reactive oxygen species; SEM, scanning electron microscopy; tBid, truncated Bid; TEM, transmission electron microscopy; TNF, tumor necrosis factor; tPA, tissue plasminogen activator; TUNEL, Terminal deoxynucleotidyl Transferase Biotin-dUTP Nick End Labeling; zVAD-fmk, *N*-benzyloxycarbonyl-Val-Ala-Asp (OMe)-fluoromethylketone.

* Tel.: +81 95 819 2421; fax: +81 95 819 2420.
*E-mail address:* ueda@nagasaki-u.ac.jp.

0163-7258/$ – see front matter © 2009 Elsevier Inc. All rights reserved.
doi:10.1016/j.pharmthera.2009.05.007

## 1. Introduction

Stroke is a major cause of death and a major factor behind people spending their life confined to bed. Stroke results in dysfunctions of motor skills, memory and sensory perception, which are caused by various kinds of ischemia leading to neuronal death. Necrotic death occurs first in the ischemic core, followed by apoptosis several days later in the region surrounding the core, referred to as the penumbra (Dirnagl et al., 1999; Lipton, 1999; Ueda & Fujita, 2004). Neuronal necrosis in the ischemic core is caused by deprivation of oxygen, glucose and some neurotrophic factors, and results in the release of cytotoxic substances, which in turn generate reactive oxygen species (ROS) (Szeto, 2006) and cause further damage to the surrounding neurons. These cytotoxic substances also activate non-neuronal cells, astrocytes and microglia and further release other types of cytotoxic molecules, such as cytokines and nitric oxide, which in turn cause neuronal apoptosis (Danton & Dietrich, 2003; Dirnagl et al., 1999; Heales et al., 1999; Nakajima & Kohsaka, 2004; Swanson et al., 2004; Lai & Todd, 2006). Considering that apoptosis has the nature of being a converging type of cell death, it is interesting to hypothesize that the neuronal death expansion by necrosis is terminated by late apoptosis. This hypothesis seems to partly contradict previous findings that apoptosis inhibitors or anti-apoptotic neurotrophins have significant, but limited, protective effects against brain damage (Cheng et al., 1998; Brines et al., 2000; Gilgun-Sherki et al., 2002; Gladstone et al., 2002). The limited effects may be attributed to the fact that neuronal apoptosis is observed at the early stage of stroke as well as at the late stage (Dirnagl et al., 1999; Lipton, 1999; Ueda & Fujita, 2004). Therefore, inhibition of necrosis seems to be preferable for rapid treatment of stroke, since the rapid treatment is currently emphasized by the efficacy of thrombolytic tissue plasminogen activator (tPA) treatments (Gladstone et al., 2002; Borsello et al., 2003; "Tissue plasminogen activator for acute ischemic stroke. The National Institute of Neurological Disorders and Stroke rt-PA Stroke Study Group", 1995). However, studies of molecules that can inhibit rapid cell death by necrosis have been desired.

## 2. Proposed mechanisms for apoptosis and necrosis

Cytotoxicity is mainly divided into two specific cell death modes, namely apoptosis and necrosis, which are distinguishable by morphological criteria. Apoptosis is a self-destructive and non-inflammatory cell death, characterized by nuclear fragmentation, chromatin condensation and membrane blebbing (Danial & Korsmeyer, 2004). Apoptosis is triggered by various stimuli, such as binding of extracellular death signals, deprivation of growth factors or treatments with cytotoxic drugs (Sprick & Walczak, 2004). In response to any kind of stimuli, activated caspases (cysteinyl aspartate-specific proteases) mediate the resulting apoptotic cell death. Activation of initiator caspases, such as caspase-8 and caspase-9, will proteolytically activate effector procaspases, which are responsible for the cleavage of vital cell components and subsequent execution of cell death. The Bcl-2 family consisting of anti-apoptotic (Bcl-2, Bcl-xL) and pro-apoptotic (Bax, Bak) proteins decides whether a cell lives or dies. In contrast to apoptosis, necrosis has traditionally been perceived as a passive form of cell death. Necrosis is bioenergetic and catastrophic (Edinger & Thompson, 2004) and lacks the characteristics of apoptotic processes. Instead, it is characterized by mitochondrial swelling, loss of electron-density and early plasma membrane rupture, leading to local inflammation. However, the molecular bases of the underlying mechanisms remain to be determined. It is only accepted that deficiency of cellular ATP determines necrotic cell death.

In addition to these representative cell death modes, a unique cell death mode, autophagy, has recently been well discussed. Autophagy is a self-destructive cell death process through a lysosomal pathway and characterized by the presence of autophagic vacuoles, designated autophagosomes (Levine & Yuan, 2005). Unlike apoptosis, autophagy principally plays a cell-adaptive role for survival or repair under stress (starvation) conditions. However, a massive autophagic process can kill damaged cells (Gozuacik & Kimchi, 2004, 2007). In this mechanism, sequestration of cellular components for recycling leads to the formation of a double-membrane autophagosome, which fuses with an endosomal vesicle and a lysosome. Depending on the cellular environment, this process is destined for either a survival or death mechanism. Most recently, the Nomenclature Committee on Cell Death (NCDD) reported updated guidelines and understanding of the various cell death modes (Kroemer et al., 2009).

### 2.1. The three major pathways of apoptosis

Regarding the mechanisms of apoptosis, the three major pathways all involve caspase-3 activation and nuclear fragmentation as the final step (Baker & Reddy, 1998; Ferri & Kroemer, 2001; Chen & Goeddel, 2002; Danial & Korsmeyer, 2004). In the first mechanism through mitochondrial pathways, release of apoptosis-initiation factors from mitochondria plays key roles in successive apoptosome formation and caspase-3 activation (Kroemer, 1997; Ferri & Kroemer, 2001; Martinou & Green, 2001; Zamzami & Kroemer, 2001). These factors, including soluble intermembrane proteins such as cytochrome *c* (Liu et al., 1996), apoptosis-inducing factor (Susin et al., 1999), Smac/DIABLO (Du et al., 2000), EndoG (Li et al., 2001) and HtrA2/Omi (Suzuki et al., 2001), are released through mitochondrial permeability transition pores (mPTPs) comprised of adenine nucleotide translocase and voltage-dependent anion channels, as shown in Fig. 1. The released cyto *c* forms an apoptosome together with procaspase-9, Apaf1 and ATP, and generates activated caspase-9, which in turn further activates caspase-3, followed by DNA fragmentation through activation of caspase-activated DNase (Enari et al., 1998; Sakahira et al., 1998). The opening of mPTPs is positively regulated by pro-apoptotic Bax and Bak, and negatively regulated by anti-apoptotic Bcl-2 and Bcl-xL (Tsujimoto, 2002; Cory et al., 2003). Consequently, these Bcl-2 family proteins play key roles in determining the mitochondrial pathway of apoptosis. There are several other Bcl-2 family proteins that can also regulate mPTP opening. Specifically, they are pro-apoptotic Bad, Bim and truncated Bid (tBid), which stimulate mPTP opening by absorbing Bcl-2 and Bcl-xL through heterodimerization (Tsujimoto, 2003). Growth factors or neurotrophic factors are known to inhibit apoptosis by activating Akt, which phosphorylates Bad and abolishes its interactions with Bcl-2 and Bcl-xL (Zha et al., 1996; Shimizu et al., 2000; Belzacq et al., 2003). Phosphorylated Bim becomes detached from microtubules and is transported to mitochondria (O'Connor et al., 1998; Chen & Zhou, 2004). Since some growth factors are also known to enhance the expression of Bcl-2 and Bcl-xL (Rodeck et al., 1997; Riccio et al., 1999; Yabe et al., 2001), this mitochondrial pathway could be closely related to the actions of growth factors. The second mechanism is mediated by death receptors, namely Fas and tumor necrosis factor (TNF)α1 receptors, which are activated by Fas ligand and TNFα, respectively. These receptors mediate the activation of caspase-8 and caspase-3 through FADD, RIP and TRADD (Ashkenazi & Dixit, 1998; Walczak & Krammer, 2000). Activation of the mitochondrial pathway is also caused by the formation of tBid through partial cleavage of Bid (Luo et al., 1998). The death receptors also mediate the activation of Jun N-terminal kinase through apoptosis signal-regulating kinase 1 (Nishitoh et al., 1998). In the third mechanism, accumulation of abnormal (misfolded) proteins in the endoplasmic reticulum (ER) initiates the so-called ER stress, which leads to cleavage and activation of IRE1α/β and caspase-12 (caspase-4 in humans) (Nakagawa et al., 2000; Diaz-Horta et al., 2002), followed by activation of TRAF-2 and caspase-3, respectively (Urano et al., 2000; Yoneda et al., 2001; Nishitoh et al., 2002).

### 2.2. Necrosis mechanisms

Although the molecular mechanisms underlying necrosis remain to be fully clarified, it is now accepted that energy failure, or a drastic

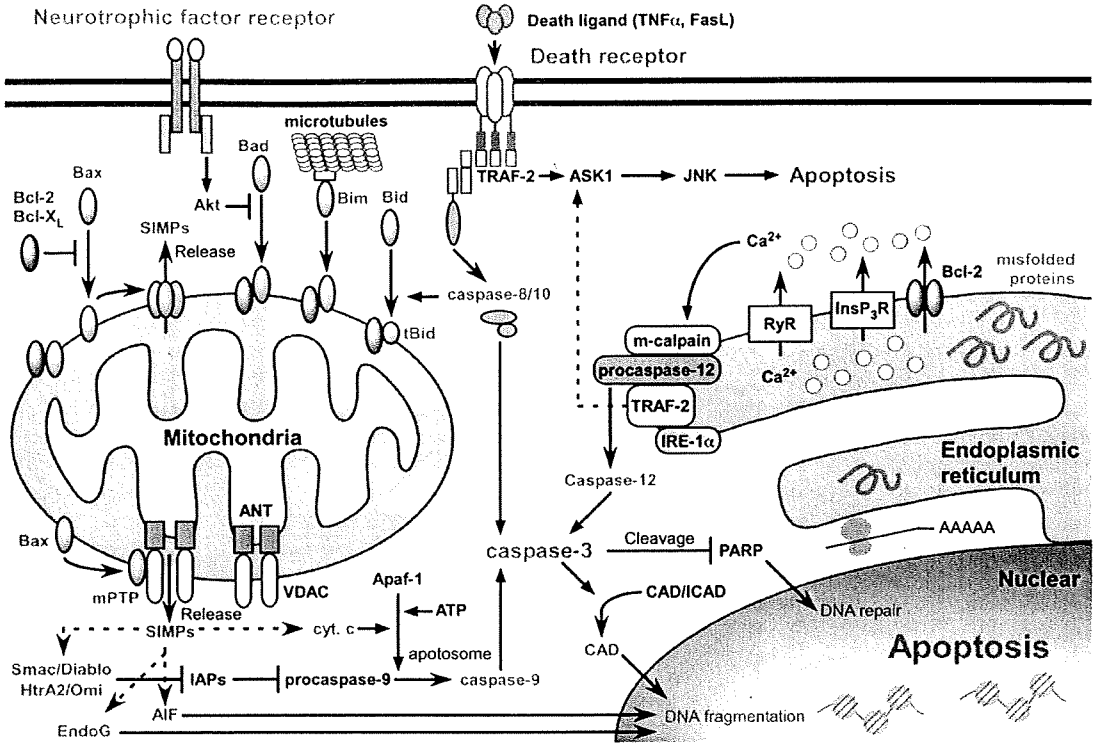


**Fig. 1.** The three major pathways of apoptosis. Mitochondrial pathways are closely related to the expression of members of the Bcl-2 family of proteins. Pro-apoptotic Bak and Bax open mitochondrial permeability transition pores (mPTPs) to release soluble intermembrane proteins (SIMPs) including cytochrome c (cyt.c), apoptosis-inducing factor (AIF), Smac/DIABLO, EndoG and HtrA2/Omi. Among these, cyt.c plays a major role in inducing apoptosis through activation of caspase-3 and caspase-activated DNase (CAD). Bcl-2 and Bcl-XL are major anti-apoptotic proteins that inhibit the functions of these pro-apoptotic proteins. The other two pathways through death receptors (FAS and tumor necrosis factor (TNF)α receptors) or endoplasmic reticulum stress also use caspase-3 activation as the common execution pathway. Other details are described in the text.

decrease in the cellular ATP levels is the most likely mechanism (Eguchi et al., 1997; Leist et al., 1997). Three major parameters, namely supply, synthesis and consumption, are known to determine the cellular ATP levels (Fig. 2). Glucose uptake through glucose transporters plays key roles in the supply of cellular glucose and ATP production. It is well known that insulin receptors mainly determine glucose uptake by recruiting the glucose transporters GLUT1 and GLUT4 (GLUT1/4) to the plasma membrane through phosphorylation in peripheral cells (Ducluzeau et al., 2002). In contrast, glucose supply in neurons is mediated by transporters that are constitutively expressed in the membranes as well as neurotrophin-regulated transporters (Cheng et al., 2000; Burkhalter et al., 2003).

The relationship between decreased glucose uptake (supply) and necrosis induction has recently been proven in a characteristic model of neuronal necrosis using low-density and serum-free culture of cortical neurons (Fujita & Ueda, 2003a,b). In this extreme starvation or ischemic model, there are rapid decreases in [$^3$H]-2-deoxyglucose (DG) uptake and the cellular ATP levels, possibly due to endocytosis of GLUT1/4 under such starvation conditions. In mitochondrial ATP synthesis, generation of ROS and subsequent damage to mitochondrial membranes may cause a decrease in the synthesis. There is a recent report that BNIP3 opens mPTPs to allow mitochondrial influx of $H_2O$ and $Ca^{2+}$ (Vande Velde et al., 2000), which in turn causes activation of phospholipase A2 (PLA2) and mitochondrial membrane destruction (Malis & Bonventre, 1988). Lastly, ATP consumption may be facilitated by activation of poly (ADP-ribose) polymerase (PARP), which restores the damage to nuclear DNA caused by ROS using abundant ATP molecules. Decreased ATP levels cause $Ca^{2+}$ influx through $Na^+$–$Ca^{2+}$ exchangers owing to loss of $Na^+$–$K^+$ ATPase and reduced $Ca^{2+}$ efflux owing to loss of $Ca^{2+}$–$Mg^{2+}$ ATPase activity. Consequently, the elevated $[Ca^{2+}]_i$ activates PLA2 and leads to degradation of the plasma membrane. An osmotic problem caused by the damaged ion balance may also be involved in the membrane destruction. Hence, one of the promising strategies for inhibiting necrosis would be to increase cellular ATP levels or inhibit the rapid decrease in ATP levels in the event of necrosis. It is also interesting that caspase-3 catalyzes PARP, and thereby inhibits ATP consumption for the repair of DNA damage (Fig. 1). In other words, apoptosis mechanisms also play roles in inhibiting necrosis.

### 2.3. Morphological differences between apoptosis and necrosis

In most cells, including neurons, cell death is mainly classified into apoptosis and necrosis based on morphological characterization (Kerr et al., 1972). The morphologies of apoptosis and necrosis vary among different cells, nutrient conditions and amounts of time after stress. Fortunately, we have successfully demonstrated both cell death modes using the same cell types and the same nutrient conditions. In previous studies, cortical neurons from embryonic day 17 rat brains were cultured under serum-free conditions without any supplements (Fujita et al., 2001; Fujita & Ueda, 2003a,b). As early as 6 h, but not at 3 h, after the start of serum-free culture, neurons in low-density ($1\times10^5$ cells/cm$^2$) cultures showed many pores on their surfaces by scanning electron microscopy (SEM) analysis (Fujita & Ueda, 2003a,b; Ueda et al., 2007). At 12 h, the cell surface membranes were largely destroyed and only the nuclei remained. By transmission electron microscopy (TEM) analysis, typical necrotic features, such as membrane destruction, loss of cytoplasmic electron-density and swollen mitochondria with a disrupted cristae structure, were observed at 6 h (Fujita & Ueda, 2003a,b). These features represent typical necrosis. When high-density ($5\times10^5$ cells/cm$^2$) cultures were analyzed by SEM, the neurons initially

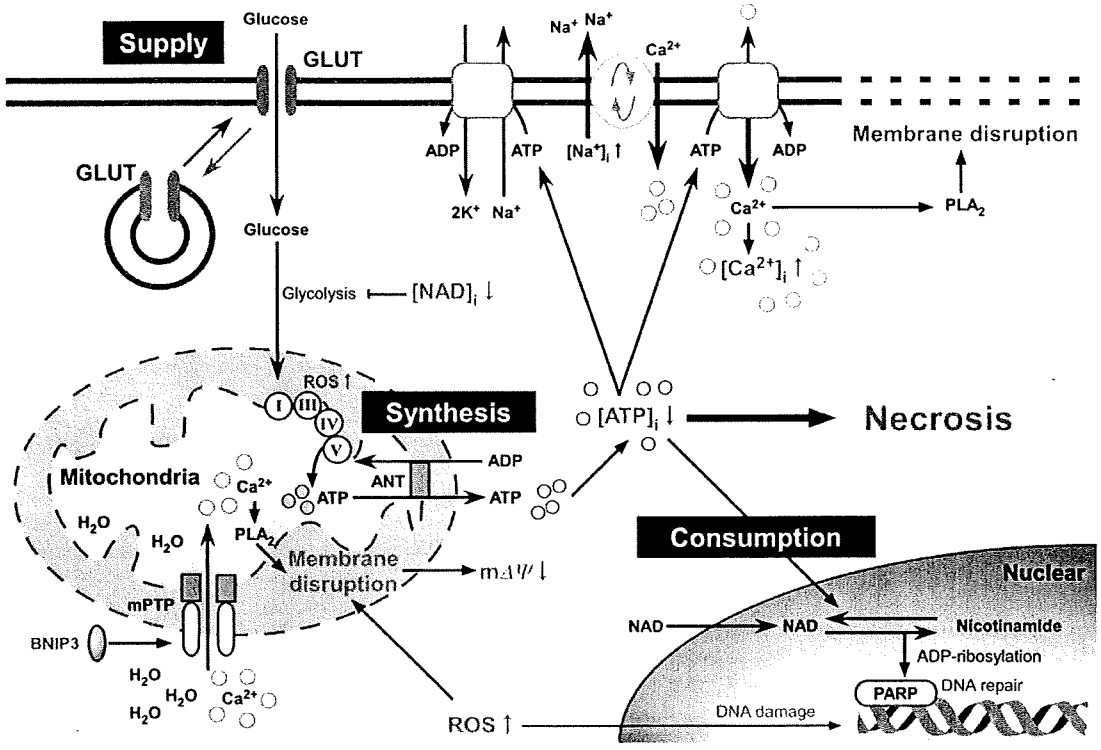


**Fig. 2.** Roles of ATP metabolism in neuronal necrosis. Glucose transporters (GLUTs) are involved in the supply of cellular glucose (depicted as supply), a substrate for ATP production through glycolysis and oxidative phosphorylation (depicted as synthesis) in mitochondria. Some species of GLUT are constitutively localized, while others are translocated to the membrane upon cell stimulation by extracellular signals. Poly (ADP-ribose) polymerase (PARP) restores the DNA damage caused by cellular stress, by using abundant cellular ATP molecules (depicted as consumption). A rapid decrease in the cellular ATP levels leads to necrosis.

showed a smooth cell surface and subsequently exhibited some blebbing on the surface at 12 h after the start of serum-free culture (Fujita & Ueda, 2003a,b). On the other hand, TEM analysis revealed that the cells exhibited split nuclei and chromatin condensation, with no significant damage to the mitochondria. All these features represent typical apoptosis.

## 3. Necrosis models for primary culture of cortical neurons

Most types of vertebrate cells other than blastomeres are considered to require continuous signals from other cells to survive (Raff, 1992). For survival in vivo, neurons also require various signals from target tissues, glial cells or other neurons via synapses. Although neurotrophic factors are known to be signals that promote neuronal survival, neurons at the early stage of development must survive in the absence of such neurotrophic factors from glial cells or synapses (Davies, 1994). Indeed, neurons can survive in culture conditions under high-$K^+$ stimulation without serum (Scott & Fisher, 1970). To investigate whether neurons can survive without any signals from other cell types or the environment, we previously attempted to characterize neuronal survival activity under serum-free conditions without any exogenous signal molecules (Fujita et al., 2001). We found that cortical neurons under serum-free conditions died by necrosis in low-density cultures. Notably, however, the neurons died by apoptosis in high-density cultures. These findings suggest that some soluble factors in the high-density cultures may switch the cell death mode from necrosis to apoptosis.

### *3.1. Characterization of neuronal necrosis in low-density and serum-free culture*

To study the mechanisms of necrosis and search for soluble factors that inhibit necrosis, the development of simple and more natural in vitro assay systems for neuronal necrosis is required. A successful method to cause pure neuronal necrosis was attained by using serum-free and low-density culture without any supplements (Fujita et al., 2001; Fujita & Ueda, 2003a,b). In the protocol, cortical neurons from embryonic day 17 rat brains were seeded on poly-ornithine-coated dishes at a low density ($1 \times 10^5$ cells/cm$^2$) in the absence of serum or any supplements. As early as 6 h, but not at 3 h, after the start of serum-free culture, the neurons showed many pores on their surfaces by SEM analysis (Fujita & Ueda, 2003a,b; Ueda et al., 2007). At 12 h, the cell surface membranes were largely destroyed and only the nuclei remained. By TEM analysis, typical necrotic features, such as membrane destruction, loss of cytoplasmic electron-density and swollen mitochondria with a disrupted cristae structure, were observed at 6 h (Fujita & Ueda, 2003a,b). Necrotic features were also detected by staining with propidium iodide (PI), but not with an antibody against activated caspase-3. In this culture system, significant PI staining was observed at 3 h after the start of low-density culture and the staining showed a parallel time-course to the decrease in cell survival.

### *3.2. Neuronal necrosis models using low-oxygen and low-glucose (LOG) stress*

Following focal ischemia in the brain, the neurons adjacent to the ischemic region rapidly die by necrosis, and the dead neurons in the ischemic core are not revived. Therefore, a clinically strategic target for the prevention of disability would be the secondary necrosis in the vicinity of the initial ischemic core region. This secondary necrosis may be caused by slightly milder ischemia or various cytotoxic molecules derived from the dead cells. Since it is difficult to specify the molecules that induce the secondary necrosis, we previously used a mild ischemia (and reperfusion) model with LOG stress as an alternative protocol for reproducing the ischemia-induced secondary necrosis. In the protocol, neurons cultured in the presence of serum were

subjected to culture in balanced salt solution medium containing 1 mM glucose (1/15 of the normal concentration) and 0.4% oxygen (1/50 of the normal level) for 2 h, followed by reperfusion with normal serum-containing medium (Ueda et al., 2004, 2007). Marked neuronal necrosis without apoptosis was observed, although the percentage of cell death (60%) at 3 h after reperfusion was slightly lower than the percentage in serum-free culture (>80%) and the survival activity did not change for 12 h. This LOG-stress model is also applicable to retinal neuron–neuroblastoma hybrid N18-RE105 cells (Ueda et al., 2004, 2007). Of interest is the observation of a marked decrease in glucose transport due to excess internalization of the glucose transporters GLUT1/4 in the cortical neurons under LOG-stress conditions (Ueda et al., 2007). Although the detailed mechanisms of the GLUT1/4 internalization under starvation or ischemic conditions remain elusive, the underlying mechanisms seem to be related to the ischemia-induced deficiency of growth factors, since GLUT membrane trafficking is regulated by growth factor-related signaling pathways through Akt, PKC or Grb2–dynamin complexes (Ando et al., 1994; Watson & Pessin, 2001, 2006). Taken together, the LOG-stress model combined with measurement of GLUT translocation may facilitate the use of drug treatments to study the signal transduction of necrosis and its inhibition by endogenous and exogenous compounds.

## 4. Identification of prothymosin α (ProTα) as a necrosis-inhibitory factor

The search for necrosis-inhibitory factors was initiated by the simple observation of density-dependent survival of cortical neurons in serum-free culture. At the beginning of the search for soluble factors responsible for neuron density-dependent survival in serum-free culture (Sasaki et al., 1998; Hamabe et al., 2000), we thought that the cell death was apoptosis because typical apoptotic nuclear fragmentation was observed in a small number of dead cells, although we noticed that this apoptosis-like cell death appeared to differ from conventional apoptosis in terms of its resistance to caspase inhibitors. After careful characterization of this unique cell death, we found that the death mode of cortical neurons in serum-free culture was necrosis under low-density conditions, but apoptosis under high-density conditions (Fujita et al., 2001). Although we had already identified the presence of neuronal death inhibitor 20 (NDI20) as a soluble survival factor in conditioned medium in studies since the early 1990s, we restarted our quest for the isolation of soluble factors as anti-necrosis factors.

After various approaches, we finally discovered a simple and efficient way to obtain significant amounts of active materials through molecular weight cut-off ultrafiltration, ion-exchange filtration and SDS-PAGE separation. After SDS-PAGE, the survival activity was recovered by a protein band at 20 kDa. This protein was analyzed by matrix-assisted laser desorption/ionization-time of flight mass spectrometry (MALDI-TOF MS), and a subsequent search of the non-redundant NCBI protein database for matching peptide mass fingerprints revealed 17 peptides that were unique to rat ProTα (Ueda et al., 2007). Moreover, tandem MS analysis confirmed that the N-terminal of purified ProTα was an acetylated serine (129.612 $m/z$ vs. Ser 87.343 $m/z$), in agreement with a previous report (Pineiro et al., 2000). The structure of ProTα has several unique characteristics in that it is highly hydrophilic and acidic (pI = 3.55) owing to its abundance of glutamic and aspartic acids (50% of the total residues) in the middle part of the protein. The cluster of acidic amino acids in this region seems to resemble a putative histone-binding domain. The region does not contain any histidine, sulfated or aromatic amino acid residues. A small stretch of basic residues, corresponding to the thymic hormone thymosin α1 (28 amino acids), is found at the N-terminal, while another stretch of basic residues at the C-terminal includes a nuclear localization signal (NLS; TKKQKK). The fact that ProTα is a monomeric protein without any regular secondary structures under physiological conditions (Gast et al., 1995) may explain its poor immunogenicity, a favorable property in terms of its clinical use. Its other characteristics have been well described (Segade & Gomez-Marquez, 1999).

For biological identification, we performed several experiments using an anti-ProTα IgG (Ueda et al., 2007). When conditioned medium factors were applied to anti-ProTα IgG-conjugated beads, the eluates obtained from acid-treated beads produced a single band corresponding to recombinant ProTα on SDS-PAGE and acidic blotting. A large proportion of ProTα and the survival activity in the conditioned medium were recovered in the eluates. ProTα purified to homogeneity exhibited an equivalent concentration-dependency to that of the recombinant protein, while ProTα mutants lacking the N-terminal region (Δ1–29) including thymosin-$\alpha_1$ (Pineiro et al., 2000) or C-terminal region (Δ102–112) including the NLS retained the original activity of ProTα.

It is often difficult to detect ProTα by SDS-PAGE analysis. Blotting onto a membrane and detection by silver staining are extremely ineffective, since ProTα is very acidic (pI = 3.75). Therefore, we often use the highly sensitive Gelcode™ Blue Stain method without a blotting procedure. On the contrary, it is very easy to purify this acidic protein. A one-step purification via acid phenol extraction of most preparations is sufficient to concentrate ProTα to a detectable level for the Gelcode™ Blue Stain method. ProTα was detected in conditioned medium as early as 1 h after the onset of serum-free and high-density culture. Since neurons in high-density culture retain intact plasma membranes at 1 h after the start of serum-free culture and ProTα lacks a signal peptide sequence required for vesicular release, it is evident that the ProTα release occurs in a regulated and unique non-classical manner (Matsunaga & Ueda, 2006a,b). However, no ProTα release was observed in the presence of serum. Taken together, these findings suggest that ProTα may play an important neuroprotective role in the event of starvation or ischemic stress.

## 5. Cell death mode switch in cultured neurons

Based on the original findings that cortical neurons show cell density-dependent survival under serum-free starvation conditions, ProTα was identified as a necrosis-inhibitory molecule. However, since neurons in high-density culture die by apoptosis, we needed to characterize the mechanisms underlying the more complicated cell death mode switch by using ProTα.

### 5.1. Inhibition of necrosis by prothymosin α

Recombinant ProTα reversed the rapid decrease in survival of cortical neurons observed in serum-free and permanent ischemia models (Ueda et al., 2007). The addition of ProTα abolished the typical necrosis features, such as disrupted plasma membranes and swollen mitochondria in TEM analysis at 6 h, but caused apoptosis at 12 h instead. When the cell death mode was evaluated by double staining with PI (necrosis)/annexin V (apoptosis at 3 h), PI/anti-activated-caspase-3 IgG (apoptosis at 12 h) and PI/TUNEL (apoptosis at 24 h), most of the neurons were found to die by necrosis under serum-free stress. Addition of ProTα totally switched the cell death mode from necrosis to apoptosis. These findings are consistent with previous studies (Fujita & Ueda, 2003a,b), in which conditioned medium derived from high-density cultures under serum-free conditions caused this type of cell death mode switch. Pharmacological studies further revealed that the survival activity of recombinant ProTα is mediated through activation of phospholipase C (PLC) and protein kinase C (PKC)β (Ueda et al., 2007), consistent with the case for the conditioned medium (Fujita and Ueda, 2003b). All of these findings strongly support that the soluble survival factor in the conditioned medium is ProTα, and that this protein causes the cell death mode switch.

Compared with the abundant reports regarding the molecular mechanisms of apoptosis (Nagata, 1997; Adams & Cory, 1998; Ashkenazi & Dixit, 1998; Evan & Littlewood, 1998; Green & Reed, 1998), little is